EcoState: Extending Ecopath with Ecosim to estimate biological parameters and process errors using RTMB and time-series data

Running title: EcoState: a state-space ecosystem model

James T. Thorson[1,*], Kasper Kristensen[2], Kerim H. Aydin[1], Sarah K. Gaichas[3], David G. Kimmel[4], Elizabeth A. McHuron[5], Jens M. Nielsen[4,5], Howard Townsend[6], George A. Whitehouse[1,5]

[1] Resource Ecology and Fisheries Management, Alaska Fisheries Science Center, National Marine Fisheries Service, NOAA

[2] Technical University of Denmark, Charlottenlund Slot Jægersborg Allé 1, 2920 Charlottenlund, Denmark

[3] Ecosystem Dynamics and Assessment Branch, Northeast Fisheries Science Center, National Marine Fisheries Service, NOAA, 166 Water Street, Woods Hole, MA, USA

[4] Resource Assessment and Conservation Engineering, Alaska Fisheries Science Center, National Marine Fisheries Service, NOAA

[5] Cooperative Institute for Climate, Ocean, and Ecosystem Studies, University of Washington, Seattle, WA, USA

[6] Marine Ecosystems Division, Office of Science and Technology, National Marine Fisheries Service, Silver Spring, MD, United States

* Corresponding author: James.Thorson@noaa.gov

Abstract:

Mass-balance ecosystem models including Ecopath with Ecosim (EwE) are widely used tools for analyzing aquatic ecosystems to support strategic ecosystem-based management. These models are typically developed by first tuning unknown parameters to achieve mass balance (termed "Ecopath"), then projecting dynamics over time ("Ecosim") while sometimes tuning predator-prey vulnerability parameters to optimize fit to available time-series. By contrast, population-dynamics (stock assessment) and multi-species models typically estimate a wide range of biological rates and parameters via their fit to time-series data, assess uncertainty via a statistical likelihood, and increasingly include process errors as "state-space models" to account for nonstationary dynamics and unmodeled ecosystem variables. Here, we introduce a state-space model "EcoState" (and associated R-package) that estimates parameters representing mass-balance dynamics directly via their fit to time-series data (absolute or relative abundance indices and fisheries catches) while also estimating the magnitude of process errors using RTMB. A case-study demonstration focused on Alaska pollock (*Gadus chalcogrammus*) in the eastern Bering Sea suggests that fluctuations in krill consumption are associated with cycles of increased and decreased pollock production. A self-test simulation experiment confirms that estimating process errors can improve estimates of productivity (growth and mortality) rates. Overall, we show that state-space mass-balance models can be fitted to time-series data (similar to surplus production stock assessment models), and can attribute time-varying productivity to both bottom-up and top-down drivers including the contribution of individual predator and prey interactions.

46 Keywords: Ecopath with Ecosim; state-space model; process errors; eastern Bering Sea; Alaska
47 pollock; mass-balance model
48

Introduction

Ecosystem-based fisheries management (EBFM) has been adopted as a policy goal for ocean management agencies worldwide (FAO 2003; European Commission 2013; NOAA 2016), and ecosystem models are an essential tool for evaluating tradeoffs among alternative management scenarios within EBFM. There are many types of ecosystem models (Hollowed et al. 2000; Plagányi 2007; O'Farrell et al. 2017), but one common strategy involves modelling consumption rates to predict changes in natural mortality and/or individual growth rates for modeled functional groups. In particular, mass-balance models track the flow of biomass among producers, consumers, predators, and fisheries (among other potential variables). The mass-balance model Ecopath (Polovina 1984) is a foundational example of mass-balance models, and it represents ecosystem structure by tracking flows between biomass pools given input parameters for initial biomass, production/biomass ratio, consumption/biomass ratio, diet composition, and fishery removals for each biomass pool. Input parameters are estimated outside the modeling framework and entered as known values using information from fishery independent surveys, fishery dependent sampling, and literature review. Because parameters come from a variety of disparate sources, it is often necessary to further tune input parameters to achieve conditions where no group has more removals (consumption and fishing) than production (i.e., "balance the model"). Guidelines are widely available for defining consumption per biomass (Palomares and Pauly 1998), production per biomass (Allen 1971), and for assessing the plausibility of a proposed Ecopath model (Link 2010). Ecopath can then be used to quantify ecosystem stability, optimum fisheries yield, and other metrics of ecosystem structure (Christensen and Walters 2004).

Mass-balance models were subsequently extended to projected dynamics forward in time given observed fishing rates or under hypothetical management scenarios. In particular, Ecosim (Walters et al. 1997; Pauly et al. 2000) recast Ecopath as a set of differential equations, and the resulting Ecopath with Ecosim (EwE) software remains one of the most widely-used ecosystem modelling platforms in the world (Colléter et al. 2015). The Ecopath mass balance is used to initialize the deterministic dynamic model Ecosim by deriving growth efficiency (initial ratio of production to consumption) and unobserved mortality parameters (initial production times the fraction of production not consumed by predators or removed by fishing). To promote ecosystem stability, Ecosim incorporates a functional response based on "foraging arena theory" (Walters et al. 1997), where predators can only forage upon an accessible fraction of prey as determined by vulnerability parameters (Ahrens et al. 2012). Ecosim projections therefore depend upon (and are sensitive to) both the input Ecopath mass-balance parameters and the vulnerability parameters governing the functional response (Gaichas et al. 2012). Ecosim vulnerability parameters are sometimes tuned via fit to predator-prey time-series (Scott et al. 2016; Bentley et al. 2024). However, time-series predictions of biomass are only calculated when tuning Ecosim, so this two-stage approach precludes using time-series data to tune the mass-balance parameters in Ecopath.

Ecopath-with-Ecosim (EwE) has been used to explore potential ecosystem thresholds (Gaichas et al. 2012), compare the performance of alternative management strategies (Christensen and Walters 2004; Lucey et al. 2021), and evaluate single-species reference points (Walters et al. 2005), among many other examples. EwE has seen less use to set annual fisheries management policies (e.g., harvest limits), although examples exist for using it to modify

93 existing single-species reference points to account for species interactions (Chagaris et al. 2020;
94 Howell et al. 2021).

95 To complement "strategic advice" provided by ecosystem models such as EwE, there is
96 also increased effort to estimate time-varying parameters within single-species stock assessments
97 (Nielsen and Berg 2014). This generally involves state-space estimation (de Valpine 2002),
98 which involves estimating both measurement errors (e.g., the difference between predicted and
99 observed biomass) and process errors (e.g., variation in demographic rates). Stock assessments
100 worldwide increasingly use state-space modelling (Stock and Miller 2021), and it is viewed as an
101 essential feature for future assessment-model development (Punt et al. 2020). This increased use
102 arises in part because state-space models can mitigate the bias that otherwise results from
103 treating some time-varying process as if it was stationary in time (Xu et al. 2020; Stock et al.
104 2021). State-space models require estimating the variance of random effects simultaneously
105 with other parameters, and therefore also requires jointly calculating the likelihood of data given
106 fixed and random effects as well as the probability of random effects given any hyperparameters
107 (Thorson and Minto 2015).

108 Statistical multispecies models (a.k.a. multispecies statistical catch-at-age) provide an
109 alternative to whole-of-ecosystem models (e.g., EwE) and state-space population models for
110 modelling populationand community dynamics. For example, CEATTLE (Jurado-Molina et al.
111 2005; Holsman et al. 2016) and GADGET (Begley and Howell 2004) both fit to survey and
112 fisheries data for multiple interacting species, while tracking how predation affects natural
113 mortality for those modeled prey species. These models serve as a useful middle-ground
114 between whole-of-ecosystem and single-species stock assessment models; they provide more
115 statistical rigor than EwE by using maximum likelihood or Bayesian methods to fit to time-series

116 data (with associated asymptotics and confidence-interval performance), while still tracking top-
117 down (predatory) control of prey species by tracking consumptive interactions. However,
118 statistical multispecies models typically do not model the impact of prey availability on predator
119 growth or survival (termed "bottom-up control"), and therefore cannot account for how changes
120 in forage availability may affect the productivity of commercially important consumers.

121 In this study, we introduce the first (to our knowledge) example of fitting a state-space
122 mass-balance ecosystem model to time-series data, including abundance indices and fishery
123 catches. To do so, we adapt the dynamics specified by Ecopath and Ecosim but use RTMB
124 (Kristensen 2024b) to implement automatic differentiation and fit process errors via maximum
125 marginal likelihood. We estimate equilibrium population biomass, nonequilibrium initial
126 conditions, catchability coefficients, the variance of process errors via fit to available time-series,
127 as well as other potential parameters (e.g., predator-prey vulnerability). We distribute our code
128 as an R package *EcoState*, initially available on GitHub (https://github.com/James-Thorson-
129 NOAA/EcoState) with full function documentation and user vignettes, and intended for
130 distribution via CRAN upon full release. We use real-world data from the eastern Bering Sea to
131 develop a "minimal realistic model" including 10 functional groups and one detrital pool (11
132 variables) centered on prey, competitors, and predators for Alaska pollock (*Gadus*
133 *chalcogrammus*). This case-study suggests that fluctuations in krill are associated with cycles of
134 lower or higher productivity for pollock. We also use a simulation experiment involving pelagic
135 primary producer, demersal detritus, two consumers, and two predators to confirm that we can
136 recover true parameters with reasonable statistical accuracy and precision. Finally, we conclude
137 by discussing directions for future developments of state-space whole-of-ecosystem models, and
138 how these models compare with state-space surplus production models.

Methods

EcoState is a mass-balance model that can be solved for equilibrium mass of different ecosystem components (e.g., detritus, primary producers, consumers, and predators) that are coupled via consumption, production, and detrital production/decomposition rates (Polovina 1984). EcoState tracks mass-vector $\boldsymbol{\beta}$ composed of mass β_s for each functional group or detrital pool (called "variables" in the following), indexed by $s \in \{1,2,\ldots,S\}$ where S is the total number of variables. Each variable is then specified as an (1) autotroph (i.e., primary producer), (2) heterotroph (i.e., consumer or predator), or (3) detritus. We attempt to use mathematical notation following guidelines from Edwards and Auger-Méthé (2019), particularly by using Greek letters for state-variables (e.g., biomass), Roman for parameters and data, vector-matrix notation (i.e., lowercase italic for scalars), and avoiding the use of multiple letters for a single parameter. This results in some departures from previous Ecopath and Ecosim notation (see Table S1 for a summary of all notation), although we use similar symbols where practical. We refer to the combination of autotrophs and heterotrophs as "biomass" or "taxa," and we also index variables as prey $i \in \{1,2,\ldots,S\}$ and predator $j \in \{1,2,\ldots,S\}$ in expressions where prey and predators are both included. Each variable s is assumed to have a fixed ratio of production to biomass p_s, consumption to biomass w_s (where $w_s = \text{NA}$ for detritus and primary producers), and a fixed $S \times S$ diet matrix $\mathbf{D}$ containing the proportion $d_{i,j}$ of diet provided by each potential prey i for predator j (where $d_{i,j} = 0$ for detritus and primary producers as "predators" j and all "prey" i). Finally, each variable is assumed to have mass that is "used" in the system (i.e., consumed by predators or removed by fisheries), and this is represented as ecotrophic efficiency e_s.

Mass-balance based on Ecopath

Similar to Ecopath, equilibrium in EcoState occurs for each variable when its gain matches loss rate. To match notation that is common in stock-assessment models, we define equilibrium mass $\bar{\beta}_s$ as the average mass in the absence of fishing:

$$\underbrace{\bar{\beta}_i}_{\substack{\text{Equilibrium} \\ \text{biomass for prey i}}} \times \underbrace{p_i}_{\substack{\text{Prey} \\ \text{production} \\ \text{per biomass}}} \times \underbrace{e_i}_{\substack{\text{Prey} \\ \text{ecotrophic} \\ \text{efficiency}}} \tag{1}$$

$$= \sum_{j=1}^{S} \left(\underbrace{d_{i,j}}_{\substack{\text{Proportion of} \\ \text{diet for predator} \\ j \text{ by prey } i}} \times \underbrace{\bar{\beta}_j}_{\substack{\text{Equilibrium} \\ \text{biomass for} \\ \text{predator } j}} \times \underbrace{w_j}_{\substack{\text{Predator} \\ \text{consumption} \\ \text{per biomass}}} \right)$$

Later, we then incorporate fishing mortality to project ecosystem dynamics away from this unfished equilibrium. Unknown values in Eq. 1 can be solved by re-expressing it in vector-matrix notation. Specifically, gains (left side of Eq. 1) are written as $\boldsymbol{\beta} \odot \mathbf{p} \odot \mathbf{e}$, where e.g. $\boldsymbol{\beta} \odot \mathbf{p}$ is the Hadamard (elementwise) product of two vectors $\boldsymbol{\beta}$ and $\mathbf{p}$. Similarly, losses (right side of Eq. 1) are s $\mathbf{D}(\boldsymbol{\beta} \odot \mathbf{w})$. Equilibrium biomass $\overline{\boldsymbol{\beta}}$ is achieved when these rates match, i.e. $\overline{\boldsymbol{\beta}} \odot \mathbf{p} \odot \mathbf{e} = \mathbf{D}(\overline{\boldsymbol{\beta}} \odot \mathbf{w})$, which can be solved for some combination of equilibrium biomass $\overline{\boldsymbol{\beta}}$ and ecotrophic efficiency (Supplementary Materials 2). Given this equilibrium, we calculate equilibrium consumption $\bar{\mathbf{C}}$:

$$\bar{\mathbf{C}} = \mathbf{D} \odot \left(\mathbf{1} \left(\overline{\boldsymbol{\beta}} \odot \mathbf{w} \right)^{\boldsymbol{T}} \right) \tag{2}$$

where $\mathbf{1}$ is a column-vector of 1s such that $\mathbf{1}^T \left(\overline{\boldsymbol{\beta}} \odot \mathbf{w} \right)$ is a matrix of equilibrium consumption $\overline{\boldsymbol{\beta}} \odot \mathbf{w}$ for each predator, repeated as separate rows for each prey.

The fitted model can then be used to solve for equilibrium levels of a specified tracer y_s for each taxon s. For example, trophic level is defined such that $\mathbf{z} = \mathbf{z}\mathbf{C}^* + \mathbf{y}$, where $\mathbf{y} = \mathbf{1}$ is the increase in trophic level each time mass is consumed, and $\mathbf{C}^*$ is the consumption $c_{i,j}$ for each

prey i by each predator j, rescaled to sum to one for each predator to represent a proportion. This simultaneous equation for trophic level is then solved as $\mathbf{z} = \mathbf{1}^t(\mathbf{I} - \mathbf{C}^*)^+$, where $(\mathbf{I} - \mathbf{C}^*)^+$ is the Penrose-Moore pseudoinverse of $\mathbf{I} - \mathbf{C}^*$ and $\mathbf{1}^t$ is a row-vector of 1s. Alternatively, we define tracer $\mathbf{y}$, e.g., as an indicator vector that is 1 for the base of the pelagic food chain and 0 otherwise, and then calculate the proportion of biomass for each taxon that results from pelagic production as $\mathbf{z} = \mathbf{y}^t(\mathbf{I} - \mathbf{C}^*)^+$.

Time-dynamics based on Ecosim

After Ecopath is applied to achieve mass-balance for all species, Ecosim is separately used to simulate dynamics forward in time (Pauly et al. 2000; Christensen and Walters 2004). By contrast, EcoState uses proposed parameters to solve for missing values that achieve mass-balance, and simultaneously uses those parameters to project dynamics for all variables at times $t \in \{t_1, t_2, \ldots, T\}$ while integrating dynamics over the interval between these times (i.e., from t_1 to t_2). We discretize time into years in the following, but future research could incorporate seasonal (e.g., monthly) variation using a higher-resolution time-interval with no change in equations or code. Similarly, future research could explore how fishing mortality affects the prey production p_i and predator consumption w_i via its impact on age-structure (Aydin 2004), although we do not do so here.

Adapting notation from Lucey et al. (2020), EcoState represents similar dynamics as Ecosim by specifying a differential equation for mass:

$$\frac{d}{dt}\boldsymbol{\beta}(t) = \left(\underbrace{\mathbf{g}(t)}_{\substack{\text{Growth} \\ \text{rate}}} - \underbrace{\mathbf{m}(t)}_{\substack{\text{Natural} \\ \text{mortality} \\ \text{rate}}} - \underbrace{\mathbf{f}(t)}_{\substack{\text{Fishing} \\ \text{mortality} \\ \text{rate}}} \right) \odot \boldsymbol{\beta}_t \tag{3}$$

where $f_s(t)$ is fishing mortality rate and both growth rate $g_s(t)$ and loss rate $m_s(t)$ are calculated from annual consumption rate $\mathbf{C}(t)$, representing the mass $c_{i,j}(t)$ of prey i consumed by predator j. Future studies could include net migration, although this is often not considered in stock-assessment models and therefore ignored here as well. Consumption rate $\mathbf{C}(t)$ variation around equilibrium consumption $\bar{c}_{i,j}$ based on predator and prey mass:

$$c_{i,j}(t) = \underbrace{\bar{c}_{i,j}}_{\substack{\text{equilibrium} \\ \text{consumption rate}}} \times \underbrace{\frac{x_{i,j}\frac{\beta_j(t)}{\bar{\beta}_j}}{x_{i,j} - 1 + \frac{\beta_j(t)}{\bar{\beta}_j}}}_{\substack{\text{predator functional} \\ \text{response}}} \times \underbrace{\frac{\beta_i(t)}{\bar{\beta}_i}}_{\substack{\text{prey functional} \\ \text{response}}} \tag{4}$$

where $\mathbf{X}$ is the matrix of predator-prey vulnerability parameters containing the vulnerability $x_{i,j}$ for prey i to predator j (Aydin 2004 Eq. 1; Plagányi and Butterworth 2004). Our model for consumption (Eq. 4) does not include those processes that are eliminated using default values in EwE as implemented in the Rpath package (Lucey et al. 2020), and see Supplementary Materials 1 for more discussion. Given that diet $d_{i,j} = 0$ for each column j associated with autotrophs or detritus, consumption $\bar{c}_{i,j} = 0$ and $c_{i,j}(t) = 0$ for autotrophs and detritus as well.

Loss rates $m_s(t)$ are calculated separately for detritus and biomass variables. Specifically, loss for biomass variables (autotrophs and heterotrophs) results from consumption and unmodeled natural mortality, while loss for detritus results from consumption and a constant export rate:

$$m_s m_s(t) = \underbrace{\frac{\sum_{j=1}^{S} c_{s,j}(t)}{\beta_s(t)}}_{\text{Consumption rate}} + \begin{cases} \underbrace{p_s(1-e_s)}_{\substack{\text{Residual natural} \\ \text{mortality rate}}} & \text{if } s \text{ is autotroph or heterotroph} \\ \underbrace{v_s}_{\text{Export rate}} & \text{if } s \text{ is detritus} \end{cases} \tag{5}$$

where residual natural mortality $p_s(1 - e_s)$ accounts for predation by unmodeled taxa, senescence, and disease, and is necessary to achieve mass-balance. Similarly, v_s is detritus

export (e.g., decomposition or turnover) rate, which is defined to ensure that net detritus accumulation matches net consumption plus export at equilibrium:

$$\bar{\beta}_s v_s = \underbrace{\sum_{i=1}^{S}\sum_{j=1}^{S} u_j \bar{c}_{i,j}(t) + \sum_{j=1}^{S} \bar{\beta}_j p_s (1 - e_s)}_{\text{Detritus accumulation}} - \underbrace{\sum_{j=1}^{S} \bar{c}_{s,j}(t)}_{\substack{\text{Detritus} \\ \text{consumption}}} \quad (6)$$

where u_j is the proportion of consumption that is not assimilated for predator j (with $u_j = 0.2$ by default) such that total unassimilated consumption $\sum_{i=1}^{S}\sum_{j=1}^{S} u_j c_{i,j}(t)$ then accumulates as detritus. Similarly, $\sum_{s=1}^{S} p_s(1 - e_s)$ is the total residual natural mortality, which we assume flows to detritus following Walters et al. (1997).

Gain rate $g_s(t)$ is then calculated differently for producers, consumers, and detritus:

$$g_s(t) = \begin{cases} \dfrac{p_s}{w_s} \times \dfrac{\sum_{i=1}^{S} c_{i,s}(t)}{\beta_s(t)} & \text{if } s \text{ is heterotroph} \\ \dfrac{p_s \bar{\beta}_s}{\beta_s(t)} \times \dfrac{x_{s,s} \dfrac{\beta_s(t)}{\bar{\beta}_s}}{x_{s,s} - 1 + \dfrac{\beta_s(t)}{\bar{\beta}_s}} & \text{if } s \text{ is autotroph} \\ \dfrac{\sum_{i=1}^{S}\sum_{j=1}^{S} u_j c_{i,j}(t) + \sum_{j=1}^{S} \beta_j(t) p_j (1 - e_j)}{\beta_s(t)} & \text{if } s \text{ is detritus} \end{cases} \quad (7)$$

where the gain rate for heterotrophs is calculated as total consumption across all prey divided by predator biomass, and multiplied by the ratio of production per biomass and consumption per biomass (termed growth efficiency). Alternatively, autotrophs do not consume other modeled taxa, so their density-dependence is modeled via a Michaelis-Menton (a.k.a. half-saturation) function (Walters et al. 1997 Eq. 5; Gaichas et al. 2012 Eq. 6) where $p_s \bar{\beta}_s$ is their equilibrium production and $\frac{x_{s,s} \frac{\beta_s(t)}{\bar{\beta}_s}}{x_{s,s} - 1 + \frac{\beta_s(t)}{\bar{\beta}_s}}$ has the same form as the predator functional response for heterotrophs (Eq. 4). Finally, detritus accumulates from the unassimilated consumption for all predators and

prey $\sum_{i=1}^{S}\sum_{j=1}^{S} u_j c_{i,j}(t)$, as well as unmodeled mortality rate $\sum_{j=1}^{S} \beta_j(t) p_j(1-e_j)$ for each taxon as prey (Walters et al. 1997).

Finally, EcoState estimates an instantaneous fishing mortality rate for any variable with catch data in a given year. To do so, EcoState tracks the harvest η_s for each variable s, and treats vector $(\boldsymbol{\beta}, \boldsymbol{\eta})$ of length $2S$ as the augmented set of state variables. Harvest is itself calculated from fishing mortality rates $\boldsymbol{\phi}(t)$ composed of $\phi_k(t)$ for each fishery k, where each fishery has species selectivity $r_{s,k}$ such that the fishing mortality rate for each species is $\mathbf{f}(t) = \mathbf{R}\boldsymbol{\phi}(t)$. We also include an additional process-error term $\boldsymbol{\epsilon}(t) \odot \boldsymbol{\beta}(t)$, where $\epsilon_s(t)$ represents unmodeled variation in population growth rates for taxon s.

$$\frac{d}{dt}\boldsymbol{\beta}(t) = \left(\underbrace{\mathbf{g}(t)}_{\substack{\text{Growth}\\ \text{rate}}} - \underbrace{\mathbf{m}(t)}_{\substack{\text{Natural}\\ \text{mortality}\\ \text{rate}}} - \underbrace{\mathbf{f}(t)}_{\substack{\text{Fishing}\\ \text{mortality}\\ \text{rate}}} + \underbrace{\boldsymbol{\epsilon}(t)}_{\substack{\text{Process error}\\ \text{in biomass rate}}} \right) \odot \boldsymbol{\beta}_t \tag{8}$$

$$\frac{d}{dt}\boldsymbol{\eta}(t) = \mathbf{f}(t) \odot \boldsymbol{\beta}(t)$$

Including process errors $\epsilon_{s,t}$ in the differential equation for mass (Eq. 8) implies that mass-balance is maintained on average over time, but not exactly in any single year. We interpret any short-term departure from mass-balance as representing processes that are not well approximated in the model, i.e., annual variation in ecotrophic efficiency, detrital export, growth efficiency, etc. resulting from unmodeled environmental conditions.

Model fitting

To fit this model, EcoState defines a set of coefficients $\boldsymbol{\theta} = (\mathbf{p}, \mathbf{w}, \mathbf{D}, \bar{\boldsymbol{\beta}}, \boldsymbol{\phi}(t), \boldsymbol{\delta}, \boldsymbol{\epsilon}(t), \mathbf{q}, \boldsymbol{\sigma}^2, \boldsymbol{\tau}^2, \boldsymbol{\nu}^2)$. These are then used to project biomass $\boldsymbol{\beta}(t)$ through time and model predictions are compared with available data to calculate a joint likelihood. We

then treat process errors $\boldsymbol{\epsilon}(t)$ as random effects, and integrate across their values using the Laplace approximation to calculate the marginal likelihood. We optimize log-marginal likelihood to identify the maximum-likelihood estimate for selected parameters. In the following, we assume that Ecopath coefficients $\mathbf{p}, \mathbf{w}$, and $\mathbf{D}$ are known, although future studies could instead specify Bayesian priors to propagate uncertainty about their values. Similarly, the user can control what combination of other parameters are estimated or fixed at known values. In particular, the user must specify a value for either ecotrophic efficiency e_s or equilibrium biomass $\bar{\beta}_s$ (but not both) for each taxon, and EcoState then solves for the unspecified value (e.g., e_s if $\bar{\beta}_s$ is treated as a parameter) for each taxon (see Supplementary Materials 2). This specified value can be fixed *a priori* (e.g., fixing ecotrophic efficiency $e_s = 1$ for a taxon s for which all predators are modeled) or estimated as a fixed effect (e.g., estimating equilibrium biomass $\bar{\beta}_s$ for a taxon that has an absolute index of biomass to inform population scale). We therefore estimate equilibrium biomass and/or ecotrophic efficiency for some set of taxa, while jointly projecting biomass $\beta_s(t)$ in discretized times $t \in \{1,2,\dots,T\}$.

We specifically assume that the biomass β_s for each variable s starts at some initial condition, $\beta_s(t_1) = \bar{\beta}_s \delta_s$, where δ_s is the ratio of initial to equilibrium mass for taxon s, where $\log(\delta_s) = 0$ by default. At the beginning of each time-interval, we similarly specify that annual harvest $\boldsymbol{\eta}(t) = \mathbf{0}$ for all taxon. We then integrate the differential equation over the interval $(t, t+1)$ using specified values of $\mathbf{p}, \mathbf{w}, \mathbf{e}, \mathbf{D}, \bar{\boldsymbol{\beta}}, \boldsymbol{\phi}(t)$ and $\boldsymbol{\epsilon}(t)$, and record the integrated value $\boldsymbol{\eta}(t+1)$ at the end of each interval as the predicted catch occurring for each taxon in that interval from t to $t+1$. In the following, we specifically use a third-order Adams-Bashford-Moulton method, but also provide an alternative fourth-order Runge-Kutta method where both are adapted from the *pracma* package in R (Borchers 2023). We initially explored alternative

ordinary differential equation (ODE) solvers that are provided by the *deSolve* package in R (Soetaert et al. 2010) using package *RTMBode* (Kristensen 2024a), but found that this approach was not sufficiently flexible to deal with the Laplace approximation given the specified structure of EcoState. We continue this integration for all $t \in \{1,2,\ldots,T\}$, while recording biomass $\boldsymbol{\beta}(t)$ and harvest $\boldsymbol{\eta}(t)$ at the end of each year. We then calculate the joint likelihood by specifying that biomass measurements follow a lognormal distribution:

$$\log(b_s(t)) \sim \text{Normal}(\log(q_s \beta_s(t)), \sigma_s^2) \quad (9)$$

where q_s is the catchability coefficient representing the proportion of biomass that is available to a monitoring program for taxon s, σ_s^2 is a user-specified variance for the any biomass measurements, and where $b_{s,t} = \text{NA}$ ignores this component from the likelihood. Similarly, we specify a lognormal distribution for catches:

$$\log(h_s(t)) \sim \text{Normal}(\log(\eta_s(t)), \nu_s^2) \quad (10)$$

where ν_s^2 is a user-specified variance for the any catch data, and where $h_s(t) = \text{NA}$ ignores this component from the likelihood. Finally, we specify a distribution for process errors:

$$\epsilon_s(t) \sim \text{Normal}(0, \tau_s^2) \quad (11)$$

where τ_s^2 and $\boldsymbol{\epsilon}_s$ can be fixed at zero *a priori* to "turn off" process errors for any taxa s, or τ_s^2 can be estimated as a fixed effect and $\boldsymbol{\epsilon}_s$ as a random effect.

EcoState is implemented in the R statistical environment (R Core Team 2023) using RTMB (Kristensen 2024b). RTMB provides a simplified interface to the Template Model Builder library (Kristensen et al. 2016), which uses automatic differentiation (AD) for efficient calculation of model derivatives. Specifically, AD allows us to efficiently compute the Laplace method to approximate the log-marginal likelihood. We then identify the maximum likelihood estimate (MLE) for fixed effects by optimizing this log-marginal likelihood, and then compute

Empirical Bayes predictions of random effects by optimizing the joint likelihood with respect to random effects using the MLE for fixed effects. Finally, we use a generalization of the delta method to compute standard errors and predictive errors for fixed and random effects (Kass and Steffey 1989). We check model convergence by confirming that: (1) the gradient of the log-marginal likelihood with respect to each fixed effect is less than 0.001; (2) the matrix of 2nd derivatives of the negative log-marginal likelihood (the outer Hessian matrix) is positive definite; and (3) the results are unchanged when increasing the number of subintervals evaluated when applying the ODE solver for Eq. 9.

EcoState has several advantages relative to previous Ecopath-with-Ecosim (Christensen and Walters 2004) or Rpath (Lucey et al. 2020) implementations of mass-balance models:

1. *Joint modelling*: It combines the mass-balance done by Ecopath with the dynamical projection from Ecosim within a single statistical model. It therefore replaces a 2-stage workflow with a single model, and allows the model to be easily refitted (including rebalancing the population scale) when adding/dropping taxa or data. Ecosim has previously been fitted to estimate vulnerability parameters using likelihood or sum-of-squares methods (Gaichas et al. 2012; Scott et al. 2016; Bentley et al. 2024), but we do not know of efforts to jointly estimate mass-balance (Ecopath) and vulnerability (Ecosim) parameters;
2. *Process errors*: By estimating process errors, we ensure that estimated mass $\beta_{s,t}$ is shrunk towards measured values $q_s b_{s,t}$ whenever measurements are available. This then ensures that modeled consumption is shrunk towards the quantity expected given that measured mass, i.e., that systematically over- or underestimating mass for a variable relative to observations does not propagate into over- or under-estimated consumption for interacting species. For variables that have no biomass measurements, dynamics are then inferred based

311 on time-varying productivity resulting from changes in modeled consumption (and resulting
312 gain and loss rates) conditional upon those estimated process errors;
313 3. *Model bridging*: If the analyst chooses to specify all parameters and turn off process errors,
314 then dynamics will be similar to those from Ecopath and Ecosim. This then facilitates model
315 building, i.e., by starting with published EwE models and progressively "turning on"
316 different parameters and/or process errors;
317 4. *Forecast variance*: If the analyst chooses to model future years with no available data
318 regarding absolute or relative mass, they must still specify a value for catch in those future
319 years. Having done this, the model will automatically propagate uncertainty about process
320 errors $\boldsymbol{\epsilon}(t)$ and resulting uncertainty about biomass $\boldsymbol{\beta}(t)$ in those future years;
321 5. *Exploring ecosystem modules*: Finally, the analyst may want to isolate interactions among a
322 small subset of taxa ("species module;" Holt 1997). The model still estimates consumption
323 among those taxa that are retained, but typically identifies decreased ecotrophic efficiency
324 for those taxa whose predators are excluded. This addresses ongoing calls for "minimal
325 realistic models" using mass-balance dynamics (Walters et al. 1997).
326 These features are common in modern stock assessment models, but novel for mass-balance
327 ecosystem models.
328 **Case study: productivity and mortality for Alaska pollock in the eastern Bering Sea**
329 To illustrate the potential benefits of EcoState, we fit it to survey data and catches for 11
330 variables in the eastern Bering Sea from 1982-2021. This example includes major predators,
331 prey, and competitors for Alaska pollock, including three fishes (pollock; Pacific cod, *Gadus*
332 *macrocephalus*, hereafter referred to as cod; and arrowtooth flounder *Atheresthes stomias*), one
333 autotroph (pelagic producers), one detritus variable, five intermediate consumers (copepods,

krill, demersal invertebrates, benthic microbes, and other pelagic zooplankton), and one predator (northern fur seal, *Callorhinus ursinus*). We use productivity and diet parameters ($\mathbf{p}, \mathbf{w}, \mathbf{D}$, see Table S2) from previous Rpath and EwE analysis (Aydin et al. 2007; Whitehouse et al. 2021), which are aggregated using biomass-weighted averages from those models. However, we use updated consumption w_s for northern fur seals to reflect their seasonal residence in the modeled area. We do not use any information about ecosystem scale (ecotrophic efficiency e_s or equilibrium biomass $\bar{\beta}_s$) from a previous mass-balance model, to avoid "double-dipping" on data that might have informed previous models and which we also use during model fitting. We fit the model using 20 sub-intervals for the Adams-Bashforth solver per year, but confirm that results are (essentially) unchanged when increasing this to 30 sub-intervals per year.

This example estimates annual fishing mortality using catch data for the three fishes (pollock, cod, and arrowtooth founder). We assume that catches arise from three separate fisheries (i.e., the fishery selection matrix $\mathbf{R}$ is an identity matrix), and specify measurement error $\nu_s = 0.1$. We also fit to biomass time-series calculated using a design-based estimator applied to survey data from an annual bottom-trawl survey in the eastern Bering Sea (Lauth and Conner 2016), and a biomass-time series for northern fur seal (from McHuron et al. 2020), and see Supplementary Materials 3 for details. Cod and arrowtooth are bottom-associated species, and we therefore assume that the biomass time-series in the eastern Bering Sea is an absolute index of biomass (i.e., catchability coefficient $q_s = 1$). Similarly, the northern fur seal biomass index is generated from population models estimating numbers at age for St. Paul and St. George Islands (we only use values from years with direct surveys occurring at those sites), and we also assume that it is an absolute index of biomass. Given this assumption, we then estimate equilibrium biomass $\bar{\beta}_s$ and initial abundance relative to equilibrium δ_s for cod, arrowtooth, and

northern fur seal as fixed effects. By contrast, pollock has both demersal and pelagic components (Monnahan et al. 2021), so we choose to treat the bottom-trawl survey as a relative abundance index, and therefore estimate catchability q_s (which we expect will be < 1) and initial abundance relative to equilibrium δ_s. Similarly, we fit to a relative abundance index (i.e., estimating catchability coefficient q_s) for biomass indices for copepods and other pelagic zooplankton (from a fall surface trawl survey), krill (from a summer acoustics survey), and pelagic primary producers (from satellite chlorophyll-*a* concentrations averaged from May to October).

For all eight variables without an absolute biomass index, we estimate population scale by specifying that ecotrophic efficiency $e_s = 1$. This specification avoids using "expert opinion" to define the equilibrium biomass $\overline{\beta_s}$, where this expert opinion might be informed by previous EwE modelling. However, future applications could instead use Bayesian priors on ecotrophic efficiency and/or equilibrium biomass to relax the assumption that $e_s = 1$ for those eight variables. Specifying $e_s = 1$ results in all mortality being due to consumption (i.e., residual mortality $p_s(1 - e_s) = 0$), such that predator and prey are tightly coupled. For all abundance indices we specify measurement error $\sigma_s = 0.1$. We also specify vulnerability $x_{i,j} = 2$ (the default from Rpath and EwE) for all heterotrophs, and $x_{i,j} = 91$ (the upper bound from Rpath) for the autotroph. Finally, we estimate annual process errors for five taxa (pollock, cod, arrowtooth, copepods, and northern fur seal) as random effects, and estimate the standard deviation of process-error variation τ_s for each of these taxa as fixed effects.

We specifically compare estimates from three contrasting specifications of EcoState:

1. *Full*: Estimating process errors and fishing mortality, to estimate annual consumption and productivity resulting from estimated biomass for predators and prey;

2. *No process errors*: Turning off process errors, to estimate the consumption and productivity that would be expected without estimating annual variation in ecological dynamics;
3. *No catches or process errors*: Turning off process errors and ignoring fishing mortality (i.e., specifying $h_s(t) = 0$ for all taxa), to estimate the equilibrium conditions that are otherwise expected.

For each model, we record annual growth rate $g_s(t)$ and mortality rate $m_s(t)$. We use this to illustrate how variation in predators and prey has resulted in time-varying production. We also decompose growth-rate and mortality-rate per biomass into the contributions from individual predators and prey species (additive components of Eq. 8 and 6, respectively), so that we can attribute changes in production to individual prey and predators. Fitting the full model with uninformative starting values required approximately 2 hours on a standard laptop using R version 4.3.0.

Simulation experiment: estimating productivity and mortality

To explore the statistical performance of EcoState, we also conduct a "self-test" simulation experiment. This experiment involves simulating ecosystem dynamics, simulating abundance indices and catch data, refitting the model to these data, and comparing estimates with known (true) values of ecosystem variables for each of 50 simulation replicates. We specifically simulate dynamics for a fictive ecosystem involving six taxa (see Table S3): one autotroph (representing pelagic primary production), one detritus (the base of the benthic foodweb), two consumers (one pelagic and one benthic), and two predators (one pelagic and one benthic) from 1980-2020. We also specify that benthic consumers and predators have slower life-history (lower p_s and higher w_s) than their pelagic counterparts. We specify that ecotrophic efficiency $e_s = 0.9$ (i.e., 90% of biomass transfer is captured) for the producers and consumers, and that

predatorshave equilibrium biomass $\overline{\beta_s} = 1$, and then solve for equilibrium biomass for the other species (see Fig. S5). Finally, we specify a vulnerability $x_{ij} = 2$ (representing a Hollings Type-2 predator functional response) for consumers and predators, and a vulnerability $x_{ij} = 91$ (representing a close-to-constant production-per-biomass) for producers.

We then simulate an increase in fishing mortality rate for the two predators over the 40 years of simulated dynamics (see Fig. S0), and specify that process errors have a standard deviation $\tau_s = 0.1$ for primary producers and predators, and $\tau_s = 0.02$ for consumers (which are also affected by process errors in both predators and producers). We simulate abundance indices and measurements of catch for each species. We then refit the model using 10 sub-intervals of the Adams-Bashforth-Moulton ODE solver. For the "full model" we estimate the difference between equilibrium and initial biomass δ_s and the magnitude of process errors τ_s for each taxon, as well as a single vulnerability $x_{shared} = x_{ij}$ for all consumers and predators (i.e., 13 fixed effects). We compare this with a "null model" that estimates only δ_s and x_{shared} (i.e., 7 fixed effects), and ignores process errors. Finally, we compare error in estimates of model parameters, as well as annual growth rate per biomass $g_s(t)$ (Eq. 8), mortality rate per biomass $m_s(t)$ (Eq. 6), and biomass $\beta_s(t)$ between the full and null models. Each replicate of the simulation model required approximately 10 min on a standard laptop using R version 4.3.0.

Results

For the eastern Bering Sea case study, the full version of the EcoState model (i.e., including 11 variables and fitting to catches using process errors) includes both benthic and pelagic sources of production (Fig. 1 and Table S3), and has variables that range from trophic level 1 (producer and detritus) to 4.3 (northern fur seal). It estimates both decadal trends and interannual variation that is consistent with biomass surveys (Fig. 2). Major consumers (pollock and cod) show biomass

426 cycles, i.e., elevated biomass from 2000-2005 and decreased biomass from 2005-2010, followed
427 by elevated biomass from 2012-17 and subsequently lower biomass. By contrast, arrowtooth
428 flounder, northern fur seal, and zooplankton are dominated by decadal trends, i.e., arrowtooth
429 showed a large increase in biomass from 1982-1990, northern fur seal showed a progressive
430 decrease in biomass from 1995 onward, and both krill and primary producers both show a
431 pronounced decline from 2008 onward. As expected, pollock biomass is higher than the bottom-
432 trawl survey index due to an estimated catchability coefficient less than one, i.e., $\log(q_s) =$
433 -0.836, and closely fits specified catch data (Fig. S1).

434 The increasing biomass trend for arrowtooth and decreasing trend for northern fur seal
435 are largely explained by the estimated difference between initial and equilibrium biomass
436 ($\log(\delta_s) = -2.226$ and 0.27, respectively; see Table S4). As a result, the trends for these taxa
437 are also captured by models that ignore process errors, or the null model without process errors
438 or catches (Fig. 3). However, the model without process errors (blue line in Fig. 3) fails to
439 capture the biomass cycles for pollock, the trends for other zooplankton, chlorophyll, and krill,
440 and dampens the cycles for Pacific cod. Similarly, the model without process errors and catches
441 estimates lower biomass overall for zooplankton (krill, copepods, and other), pollock, and
442 benthic variables. This difference in scale arises because we specify ecotrophic efficiency $e_s =$
443 1 for these species (to avoid using auxiliary information to define their population scale).
444 Without fishery harvest, the model can decrease copepod biomass from 4 to 2 million tons while
445 still maintaining the biomass of species with indices of absolute abundance (cod, arrowtooth, and
446 northern fur seals).

447 The state-space model attributes biomass patterns to annual variation in growth $g(t)$,
448 natural mortality $m(t)$, fishing mortality $f(t)$ for the three exploited fishes (Fig. 4), and process

errors (Fig. S3). Growth exceeds natural and fishing mortality rates for arrowtooth during the initial years (1982-1995), which drives an increase in biomass, and this difference subsequently declines towards zero as population biomass stabilizes. Similarly, northern fur seals have lower growth than natural mortality, in particular from 1995-2000 and again 2005-2015, which drives a decline in biomass over time. However, biomass patterns cannot be entirely explained by changes in consumption driving growth and natural mortality. Cod and pollock have lower-than-average biomass from 2005-2010, and density dependence causes estimated growth to exceed natural mortality rates (Fig. 4); however, this density-dependent increase in productivity is offset by negative process errors $\epsilon_s(t)$ (Fig. S3), which allows the model to estimate that lower-than-average biomass persists over these years. Similarly, decadal trends for northern fur seal are driven by a sequence of positive process errors until 2000 followed by negative process errors.

The model can be used to further decompose growth and mortality rates into the contribution of individual prey and predator species, respectively (Fig. 5). This exercise shows that elevated growth rates for pollock during positive cycles (top-left panel of Fig. 5) are associated with an increased proportion of krill consumption, while the contribution of copepods to pollock growth rate has been relatively consistent over time. Predation on pollock shows a small but noticeable increase when arrowtooth biomass increased from 1982-1990 (bottom-left panel of Fig. 5). However, fluctuations in pollock mortality are largely due to changes in cannibalism from pollock and predation from cod, during their population cycles. By contrast, growth rate for cod largely follows the cycles for pollock as their major prey (red in top-right panel of Fig. 5). We do not explicitly model many predators for cod, and hence their natural mortality is largely attributed to the residual mortality that is constant over time. Finally, krill has higher growth and mortality rates than either pollock or cod due to their faster life-history,

and this means that small relative differences (e.g., changing growth $g_s(t)$ from 6 to 5.8) can still result in large absolute differences in population dynamics. However, the decline in chlorophyll biomass in 2010 (Fig. 2) is immediately apparent in decreased consumption and growth-rate for krill (Fig. 5), which is synchronous with the decrease in krill biomass around that time.

Finally, our self-test simulation experiment confirms the state-space model can accurately estimate annual growth $g(t)$ and mortality $m(t)$ components (red line in Fig. 6), and generally was more precise than a model that does not estimate process errors (blue line in Fig. 6). This difference results from the ability of the state-space model to more-accurately estimate annual variation in biomass for predators and prey, and therefore also improves the estimates of consumption $c_{s_2,s_1}(t)$ and resulting estimates of predator growth and prey mortality rates. Both the full and null models can accurately estimate the vulnerability and equilibrium biomass parameters (see Fig. S5).

Discussion

Here, we demonstrated the first (to our knowledge) state-space version of a whole-of-ecosystem model for marine ecosystems that allows for more complete and systematic estimation of process error across all species, without pre-specifying the driving processes. We extended the Ecopath-with-Ecosim model, which has over 487 models compiled online[1] and remains one of the most widely used models for ocean ecosystems worldwide (Colléter et al. 2015). EcoState specifies mass-balance dynamics using nonlinear differential equations. We integrate this differential equation over time by embedding alternative ODE solvers within a statistical language RTMB that implements automatic differentiation and uses the Laplace approximation to efficiently marginalize across random effects. Including random effects allows us to capture decadal trends

[1] As compiled on EcoBase (https://ecobase.ecopath.org/) and accessed June 11, 2024.

494 and interannual cycles in biomass (which are otherwise mis-specified in a model that does not
495 have process errors, Fig. S3), and to more accurately capture the variable growth and mortality
496 rates that result from changes in consumption. Estimating parameters via maximum likelihood
497 also allows us to propagate variance in both fixed effects (e.g., equilibrium biomass) and process
498 errors when predicting biomass in unsampled years. This predictive variance includes the
499 contribution of both fixed effects and process errors, such that biomass has higher predictive
500 uncertainty when distant from available data and/or for taxa with rapid life-histories.

501 Previous research has explored alternative methods to fit Ecosim models to time-series
502 data, and standard practice is to include time-series calibration based on tools built into EwE for
503 maximum likelihood estimation of vulnerability ($x_{i,j}$) parameters (Scott et al. 2016; Bentley et
504 al. 2024). Further, EwE includes "anomaly search" functions that either use external indices
505 (e.g. upwelling) to explain residuals in fit to time-series, or fit pre-specified types of process
506 error, for example, finding a primary productivity time series that best fits the data (Shannon et
507 al. 2008). However, these methods require pre-specifying the type of process error (e.g.
508 assuming prior to fitting that primary production is the main process driver); this could have the
509 effect of building some hypotheses for process effects into the model at the expense of others,
510 with implications for the fit and projections (Gaichas et al. 2011).

511 Our case-study involving the Bering Sea illustrates several notable patterns in this
512 ecosystem, which generates nearly 2 million metric tons of catches annually. Specifically, the
513 ecosystem includes both cyclic and long-term biomass trends that are not well captured by a
514 mass-balance model without process errors (also noted by Aydin and Mueter 2007). In
515 particular, primary producers have declined by nearly 30%, and this is synchronous with a
516 declining trend in krill biomass. Previous studies have debated the relative importance of top-

down and bottom-up control for krill biomass (Ressler et al. 2012, 2014), and our study identifies declining chlorophyll-a concentrations (and its impact on growth) as a potential mechanism (see Fig. 4 bottom-left panel). The model then attributes a small decline in productivity for pollock to this depressed krill biomass. This bottom-up impact from chlorophyll (producer) to krill (intermediate consumer) to predator (pollock) is the reverse of a trophic-cascade, wherein a change in predator abundance is predicted to impact producers (Ripple et al. 2016). These types of multi-level bottom-up impacts are not represented by statistical multispecies models, and emphasizes the importance of improved monitoring for krill in understanding climate-impacts on ecosystem productivity. However, we note that bottom-up forcing is also favored by model assumptions, i.e., assuming ecotrophic efficiency $e_i = 1$ for prey groups (thus eliminating non-predation natural mortality) and assuming that vulnerability $x_{i,j} = 2$. In particular, future studies should seek to identify whether declining primary producers is associated with an increase in consumption w_s and/or production p_s per biomass, which could offset the food-web impacts of declining primary producers (Nielsen et al. 2023).

The Bering Sea case-study illustrates how a mass-balance model can be recast using a reduced set of focal species. Recent Rpath models for the eastern Bering Sea have included nearly 100 taxa (Aydin et al. 2007; Whitehouse et al. 2021), and the resulting model is typically used to evaluate strategic (long-term) tradeoffs among management strategies. By contrast, our EcoState model includes only 10 functional groups and one detrital pool; this small size is relatively rare for mass-balance models (although see Chagaris et al. 2020), although pooling taxa still results in nearly 80% of biomass from the full Rpath model being included (see Supplementary Materials S3). Including fewer taxa allows us to calculate a high-accuracy solution to the differential equation for biomass, as required when estimating process errors. It

also allows us to provide a statistically rigorous prediction of ecosystem variables (and associated uncertainty) beyond the range of abundance indices, as desired for Models of Intermediate Complexity for Ecosystems (Plagányi et al. 2014). These predictions could then be used for seasonal-to-decadal forecasting, identifying annual status relative to ecosystem targets, or other tactical (short-term) management decisions (Plagányi 2007). Additionally, capacity constraints limit the use of ecosystem and multispecies models for short-term fisheries management. Modelers typically have just a few years to develop a "research" model and then show its usefulness for management. In that time, a model may not be used because (1) data streams were not available in a timely manner, (2) time allocated for peer review was inadequate, and (3) additional scenarios or diagnostics could not be conducted within the time allocated for peer review. Including fewer species can address these concerns by (1) reducing model implementation time as an analyst could focus on developing a smaller set of data inputs, (2) simplifying the peer review process, and 3) reducing model run time thus allowing more time for running different management scenarios. However, using a smaller set of taxa also has drawbacks, i.e., it narrows the range of alternate pathways for trophic interactions, and therefore may result in stronger predator-prey interactions than those estimated when including more taxa. In the case-study presented here, we have included major predators and prey for Alaska pollock but, e.g., a model focused on cod would need to include additional predators to better represent the residual mortality rate (Fig. 4 2nd row right column).

This state-space mass-balance model can also be interpreted as a mechanistic model to incorporate time-varying productivity into biomass-dynamic (a.k.a., surplus production) models. Biomass-dynamic models are one of the oldest models in ecology (Pearl and Reed 1920) and fisheries (Russell 1931), and state-space extensions are still widely used to identify stock status

for many fisheries worldwide (Pedersen and Berg 2017; Winker et al. 2020). These models typically estimate population scale (equilibrium biomass and a catchability coefficient) by treating the fishery as a depletion experiment (Magnusson and Hilborn 2007). We encourage future research to compare EcoState against state-space biomass-dynamics models. In particular, EcoState would provide a parsimonious approach to predict nonstationarity (in intrinsic growth rate r or equilibrium K) resulting from changing predator or prey biomass (Aydin 2004), while allowing estimates of the catchability coefficient in some cases. We hypothesize that trophic interactions could result in population-cycles that are otherwise missing from single-species biomass-dynamic models (Walters and Kitchell 2001), and could also change the shape of the production function (and resulting biological reference points).

We envision several ways that EcoState could be further advanced by future studies. Most importantly, population dynamics and statistical multispecies models typically use information about population age and size structure to better represent population lags (e.g., how changes in recruitment have a lagged effect on population biomass), nonstationary demographic rates (e.g., a lower consumption-per-biomass when average age is higher than equilibrium), and diet switching (e.g., ontogenic changes in consumptive interactions). Ecopath-with-Ecosim represents these impacts by dividing taxa into "stanzas" (multiple life-stages) for focal taxa (Christensen and Walters 2004). We recommend future research to incorporate stanzas into EcoState; we did not do this here to focus attention on the many novel aspects of our study, including (1) jointly fitting equilibrium biomass and observation errors (catchability), and (2) incorporating process errors in a nonlinear differential equation model. Similarly, future studies could include stomach-content data to identify changes in diet over time, ideally while jointly estimating the "data-weighting" for time-varying diet (Grüss et al. 2020). Finally, we

recommend continued simulation-testing of EcoState, e.g., to identify whether Bayesian priors can be used to also estimate production and consumption parameters. Such testing could be used to explore model diagnostics, both to determine when mass-balance models are likely to have good (or poor) predictive skill, or to identify when additional processes should be added (Carvalho et al. 2021).

Finally, we recommend that future studies attribute process errors to additional oceanographic, ecological, physical drivers. We have specified that process errors are independent and identically distributed, but recent research has demonstrated how to specify a dynamic structural equation model (DSEM) representing lagged and simultaneous causal effects among process errors (Thorson et al. 2024). We therefore envision that future studies could treat annual covariates (e.g., ocean temperature or predator-prey overlap) as additional model variables that are treated as measured without error, and then estimate the impact of these covariates on estimated process errors. This is somewhat akin to the "forcing functions" that are estimated using covariates in Ecopath-with-Ecosim, although DSEM would allow missing covariate values to be imputed based on temporal and multivariate correlations, similar to recent practices in stock assessment (du Pontavice et al. 2022). For example, previous research suggests that predator-prey dynamics are affected by spatial overlap by predator and prey (Goodman et al. 2022), which is in turn driven by winter sea ice production and the spatial extent of the summer "cold pool" (Thorson et al. 2021). Incorporating covariates into mass-balance models is a long-term goal for ecosystem modelers (Gaichas et al. 2011), and we suspect that combining DSEM with EcoState represents a computationally efficient and expressive interface for doing so.

Acknowledgements

We thank Sean Lucey for previous research developing Rpath, and Arnaud Grüss and Greig Oldford for helpful comments on a previous draft. Data were collected by many programs at the Alaska Fisheries Science Center, and we thank the midwater acoustics and conservation engineering (MACE) program for developing the krill index, the groundfish assessment program (GAP) for collecting the bottom-trawl survey data, the Recruitment Process Program (RPP) for collecting the copepod and other pelagic zooplankton samples, the Alaska Ecosystem Program (AEP) for collecting the northern fur seal data, and the Fisheries Monitoring and Analysis (FMA) Division for collecting fishery data that is used to estimate fishery harvest. We also thank the assessment authors for pollock (J. Ianelli), cod (S. Barbeaux), and arrowtooth (I. Spies) for prior research regarding the fished species. This publication is partially funded by the Cooperative Institute for Climate, Ocean, & Ecosystem Studies (CICOES) under NOAA Cooperative Agreement NA20OAR4320271, Contribution No. 2024-1391. [ADD CICOES contribution number]

Data Availability Statement

All data and code are included in R-package *EcoState* release 0.1.0 (https://github.com/James-Thorson-NOAA/EcoState), which is available as a public GitHub repository during review, and intended for submission to CRAN upon acceptance. *EcoState* release 0.1.0 includes three vignettes: (1) "simulation" shows how to fit the simulated 6-species ecosystem using EcoState, and contrasts it with package Rpath; (2) "surplus production" shows how to fit single-species data simulated using a Fox production function as a state-space biomass-dynamics model using EcoState, and contrasts fit with JABBA (Winker et al. 2024) and SPiCT (Pedersen and Berg 2017); (3) "eastern Bering Sea" shows how to fit the eastern Bering Sea case study involving 10 functional groups and 1 detritus pool.

Works cited

Ahrens, R.N.M., Walters, C.J., and Christensen, V. 2012. Foraging arena theory. Fish Fish. **13**(1): 41–59. doi:10.1111/j.1467-2979.2011.00432.x.

Allen, K.R. 1971. Relation Between Production and Biomass. J. Fish. Res. Board Can. **28**(10): 1573–1581. NRC Research Press. doi:10.1139/f71-236.

Aydin, K., Gaichas, S., Ortiz, I., Kinzey, D., and Friday, N. 2007. A comparison of the Bering Sea, Gulf of Alaska, and Aleutian Islands large marine ecosystems through food web modeling. U.S. Dep. Commer. Available from https://repository.library.noaa.gov/view/noaa/22894/noaa_22894_DS1.pdf.

Aydin, K., and Mueter, F. 2007. The Bering Sea—A dynamic food web perspective. Deep Sea Res. Part II Top. Stud. Oceanogr. **54**(23): 2501–2525. doi:10.1016/j.dsr2.2007.08.022.

Aydin, K.Y. 2004. Age structure or functional response? Reconciling the energetics of surplus production between single-species models and ecosim. Afr. J. Mar. Sci. **26**: 289–301.

Begley, J., and Howell, D. 2004. An overview of Gadget, the globally applicable area-disaggregated general ecosystem toolbox. ICES. Available from https://imr.brage.unit.no/imr-xmlui/bitstream/handle/11250/100625/FF1304.pdf?sequence=1 [accessed 11 June 2024].

Bentley, J.W., Chagaris, D., Coll, M., Heymans, J.J., Serpetti, N., Walters, C.J., and Christensen, V. 2024. Calibrating ecosystem models to support ecosystem-based management of marine systems. ICES J. Mar. Sci. **81**(2): 260–275. doi:10.1093/icesjms/fsad213.

Borchers, H.W. 2023. pracma: Practical Numerical Math Functions. Available from https://CRAN.R-project.org/package=pracma.

Carvalho, F., Winker, H., Courtney, D., Kapur, M., Kell, L., Cardinale, M., Schirripa, M., Kitakado, T., Yemane, D., Piner, K.R., Maunder, M.N., Taylor, I., Wetzel, C.R., Doering, K., Johnson, K.F., and Methot, R.D. 2021. A cookbook for using model diagnostics in integrated stock assessments. Fish. Res. **240**: 105959. doi:10.1016/j.fishres.2021.105959.

Chagaris, D., Drew, K., Schueller, A., Cieri, M., Brito, J., and Buchheister, A. 2020. Ecological Reference Points for Atlantic Menhaden Established Using an Ecosystem Model of Intermediate Complexity. Front. Mar. Sci. **7**. Frontiers. doi:10.3389/fmars.2020.606417.

Christensen, V., and Walters, C.J. 2004. Ecopath with Ecosim: methods, capabilities and limitations. Ecol. Model. **172**(2): 109–139. doi:10.1016/j.ecolmodel.2003.09.003.

Colléter, M., Valls, A., Guitton, J., Gascuel, D., Pauly, D., and Christensen, V. 2015. Global overview of the applications of the Ecopath with Ecosim modeling approach using the EcoBase models repository. Ecol. Model. **302**: 42–53. doi:10.1016/j.ecolmodel.2015.01.025.

du Pontavice, H., Miller, T.J., Stock, B.C., Chen, Z., and Saba, V.S. 2022. Ocean model-based covariates improve a marine fish stock assessment when observations are limited. ICES J. Mar. Sci. **79**(4): 1259–1273. doi:10.1093/icesjms/fsac050.

Edwards, A.M., and Auger-Méthé, M. 2019. Some guidance on using mathematical notation in ecology. Methods Ecol. Evol. **10**(1): 92–99. doi:10.1111/2041-210X.13105.

European Commission. 2013. REGULATION (EU) No 1380/2013 OF THE EUROPEAN PARLIAMENT AND OF THE COUNCIL. EUROPEAN PARLIAMENT AND OF THE COUNCIL, Brussels.

FAO. 2003. Fisheries management. The ecosystem approach to fisheries. UN Food and Agriculture Organization, Rome.

Gaichas, S.K., Aydin, K.Y., and Francis, R.C. 2011. What drives dynamics in the Gulf of Alaska? Integrating hypotheses of species, fishing, and climate relationships using ecosystem modeling. Can. J. Fish. Aquat. Sci. **68**(9): 1553–1578. NRC Research Press. doi:10.1139/f2011-080.

Gaichas, S.K., Odell, G., Aydin, K.Y., and Francis, R.C. 2012. Beyond the defaults: functional response parameter space and ecosystem-level fishing thresholds in dynamic food web model simulations. Can. J. Fish. Aquat. Sci. **69**(12): 2077–2094. NRC Research Press. doi:10.1139/f2012-099.

Goodman, M.C., Carroll, G., Brodie, S., Grüss, A., Thorson, J.T., Kotwicki, S., Holsman, K., Selden, R.L., Hazen, E.L., and De Leo, G.A. 2022. Shifting fish distributions impact predation intensity in a sub-Arctic ecosystem. Ecography **2022**(9): e06084. doi:10.1111/ecog.06084.

Grüss, A., Thorson, J.T., Carroll, G., Ng, E.L., Holsman, K.K., Aydin, K., Kotwicki, S., Morzaria-Luna, H.N., Ainsworth, C.H., and Thompson, K.A. 2020. Spatio-temporal analyses of marine predator diets from data-rich and data-limited systems. Fish Fish. **21**(4): 718–739. doi:10.1111/faf.12457.

Hollowed, A.B., Bax, N., Beamish, R., Collie, J., Fogarty, M., Livingston, P., Pope, J., and Rice, J.C. 2000. Are multispecies models an improvement on single-species models for measuring fishing impacts on marine ecosystems? | ICES Journal of Marine Science | Oxford Academic. ICES J. Mar. Sci. **3**(1): 707–719.

Holsman, K.K., Ianelli, J., Aydin, K., Punt, A.E., and Moffitt, E.A. 2016. A comparison of fisheries biological reference points estimated from temperature-specific multi-species and single-species climate-enhanced stock assessment models. Deep-Sea Res. Part II Top. Stud. Oceanogr. **134**: 360–378. doi:10.1016/j.dsr2.2015.08.001.

Holt, R.D. 1997. Community modules. *In* Multitrophic interactions in terrestrial ecosystems, 36th Symposium of the British Ecological Society. Blackwell Science Oxford. pp. 333–349.

Howell, D., Schueller, A.M., Bentley, J.W., Buchheister, A., Chagaris, D., Cieri, M., Drew, K., Lundy, M.G., Pedreschi, D., Reid, D.G., and Townsend, H. 2021. Combining Ecosystem and Single-Species Modeling to Provide Ecosystem-Based Fisheries Management Advice Within Current Management Systems. Front. Mar. Sci. **7**. Frontiers. doi:10.3389/fmars.2020.607831.

Jurado-Molina, J., Livingston, P.A., and Ianelli, J.N. 2005. Incorporating predation interactions in a statistical catch-at-age model for a predator-prey system in the eastern Bering Sea. Can. J. Fish. Aquat. Sci. **62**(8): 1865–1873.

Kass, R.E., and Steffey, D. 1989. Approximate Bayesian inference in conditionally independent hierarchical models (parametric empirical bayes models). J. Am. Stat. Assoc. **84**(407): 717–726. doi:10.2307/2289653.

Kristensen, K. 2024a. RTMBode: Solving ODEs with “deSolve” and “RTMB”.

Kristensen, K. 2024b. RTMB: “R” Bindings for “TMB.” Available from https://CRAN.R-project.org/package=RTMB.

Kristensen, K., Nielsen, A., Berg, C.W., Skaug, H., and Bell, B.M. 2016. TMB: Automatic differentiation and Laplace approximation. J. Stat. Softw. **70**(5): 1–21. doi:10.18637/jss.v070.i05.

Lauth, R.R., and Conner, J. 2016. Results of the 2013 eastern Bering Sea continental shelf bottom trawl survey of groundfish and invertebrate resources. NOAA Technical Memorandum, Alaska Fisheries Science Center, Seattle, WA.

Link, J.S. 2010. Adding rigor to ecological network models by evaluating a set of pre-balance diagnostics: A plea for PREBAL. Ecol. Model. **221**(12): 1580–1591. doi:10.1016/j.ecolmodel.2010.03.012.

Lucey, S.M., Aydin, K.Y., Gaichas, S.K., Cadrin, S.X., Fay, G., Fogarty, M.J., and Punt, A. 2021. Evaluating fishery management strategies using an ecosystem model as an operating model. Fish. Res. **234**: 105780. doi:10.1016/j.fishres.2020.105780.

Lucey, S.M., Gaichas, S.K., and Aydin, K.Y. 2020. Conducting reproducible ecosystem modeling using the open source mass balance model Rpath. Ecol. Model. **427**: 109057. doi:10.1016/j.ecolmodel.2020.109057.

Magnusson, A., and Hilborn, R. 2007. What makes fisheries data informative? Fish Fish. **8**(4): 337–358.

McHuron, E.A., Luxa, K., Pelland, N.A., Holsman, K., Ream, R.R., Zeppelin, T.K., and Sterling J.T. 2020. Practical Application of a Bioenergetic Model to Inform Management of a Declining Fur Seal Population and Their Commercially Important Prey. Front. Mar. Sci. doi:10.3389/fmars.2020.597973.

Monnahan, C.C., Thorson, J.T., Kotwicki, S., Lauffenburger, N., Ianelli, J.N., and Punt, A.E. 2021. Incorporating vertical distribution in index standardization accounts for spatiotemporal availability to acoustic and bottom trawl gear for semi-pelagic species. ICES J. Mar. Sci. doi:https://doi.org/10.1093/icesjms/fsab085.

Nielsen, A., and Berg, C.W. 2014. Estimation of time-varying selectivity in stock assessments using state-space models. Fish. Res. **158**: 96–101.

Nielsen, J.M., Pelland, N.A., Bell, S.W., Lomas, M.W., Eisner, L.B., Stabeno, P., Harpold, C., Stalin, S., and Mordy, C.W. 2023. Seasonal Dynamics of Primary Production in the Southeastern Bering Sea Assessed Using Continuous Temporal and Vertical Dissolved Oxygen and Chlorophyll-a Measurements. J. Geophys. Res. Oceans **128**(5): e2022JC019076. doi:10.1029/2022JC019076.

NOAA. 2016. Ecosystem Based Fisheries Management Policy of the National Marine Fisheries Service, Policy 01-120. National Oceanic and Atmospheric Administratio, Silver Spring, MD.

O'Farrell, H., Grüss, A., Sagarese, S.R., Babcock, E.A., and Rose, K.A. 2017. Ecosystem modeling in the Gulf of Mexico: current status and future needs to address ecosystem-based fisheries management and restoration activities. Rev. Fish Biol. Fish. **27**(3): 587–614. doi:10.1007/s11160-017-9482-1.

Palomares, M.L.D., and Pauly, D. 1998. Predicting food consumption of fish populations as functions of mortality, food type, morphometrics, temperature and salinity. Mar. Freshw. Res. **49**(5): 447–453. CSIRO PUBLISHING. doi:10.1071/mf98015.

Pauly, D., Christensen, V., and Walters, C. 2000. Ecopath, Ecosim, and Ecospace as tools for evaluating ecosystem impact of fisheries. ICES J. Mar. Sci. J. Cons. **57**(3): 697.

Pearl, R., and Reed, L.J. 1920. On the rate of growth of the population of the United States since 1790 and its mathematical representation. Proc. Natl. Acad. Sci. U. S. A. **6**(6): 275.

Pedersen, M.W., and Berg, C.W. 2017. A stochastic surplus production model in continuous time. Fish Fish. **18**(2): 226–243. doi:10.1111/faf.12174.

Plagányi, É.E. 2007. Models for an ecosystem approach to fisheries. Food & Agriculture Organization, Rome. Available from http://books.google.com/books?hl=en&lr=&id=MJI3aZApEQkC&oi=fnd&pg=PP9&dq=models+for+an+ecoystem+approach+to+fisheries&ots=HggvLmdgLv&sig=vCbRBUVqZlUCKnWkv8I2OVbbmRY [accessed 1 July 2012].

Plagányi, É.E., and Butterworth, D.S. 2004. A critical look at the potential of Ecopath with Ecosim to assist in practical fisheries management. Afr. J. Mar. Sci. **26**: 261–287.

Plagányi, Punt, A.E., Hillary, R., Morello, E.B., Thébaud, O., Hutton, T., Pillans, R.D., Thorson, J.T., Fulton, E.A., Smith, A.D.M., Smith, F., Bayliss, P., Haywood, M., Lyne, V., and Rothlisberg, P.C. 2014. Multispecies fisheries management and conservation: tactical applications using models of intermediate complexity. Fish Fish. **15**(1): 1–22. doi:10.1111/j.1467-2979.2012.00488.x.

Polovina, J.J. 1984. Model of a coral reef ecosystem. Coral Reefs **3**(1): 1–11. doi:10.1007/BF00306135.

Punt, A.E., Dunn, A., Elvarsson, B.Þ., Hampton, J., Hoyle, S.D., Maunder, M.N., Methot, R.D., and Nielsen, A. 2020. Essential features of the next-generation integrated fisheries stock assessment package: A perspective. Fish. Res. **229**: 105617. doi:10.1016/j.fishres.2020.105617.

R Core Team. 2023. R: A Language and Environment for Statistical Computing. R Foundation for Statistical Computing, Vienna, Austria. Available from https://www.R-project.org/.

769 Ressler, P.H., De Robertis, A., Warren, J.D., Smith, J.N., and Kotwicki, S. 2012. Developing an acoustic
770 survey of euphausiids to understand trophic interactions in the Bering Sea ecosystem. Deep Sea
771 Res. Part II Top. Stud. Oceanogr. **65–70**: 184–195. doi:10.1016/j.dsr2.2012.02.015.
772 Ressler, P.H., Robertis, A.D., and Kotwicki, S. 2014. The spatial distribution of euphausiids and walleye
773 pollock in the eastern Bering Sea does not imply top-down control by predation. Mar. Ecol. Prog.
774 Ser. **503**: 111–122. doi:10.3354/meps10736.
775 Ripple, W.J., Estes, J.A., Schmitz, O.J., Constant, V., Kaylor, M.J., Lenz, A., Motley, J.L., Self, K.E., Taylor,
776 D.S., and Wolf, C. 2016. What is a Trophic Cascade? Trends Ecol. Evol. **31**(11): 842–849. Elsevier.
777 doi:10.1016/j.tree.2016.08.010.
778 Russell, E.S. 1931. Some theoretical Considerations on the "Overfishing" Problem. ICES J. Mar. Sci. **6**(1):
779 3–20. doi:10.1093/icesjms/6.1.3.
780 Scott, E., Serpetti, N., Steenbeek, J., and Heymans, J.J. 2016. A Stepwise Fitting Procedure for automated
781 fitting of Ecopath with Ecosim models. SoftwareX **5**: 25–30. doi:10.1016/j.softx.2016.02.002.
782 Shannon, L.J., Neira, S., and Taylor, M. 2008. Comparing internal and external drivers in the southern
783 Benguela and the southern and northern Humboldt upwelling ecosystems. Afr. J. Mar. Sci.
784 Taylor & Francis Group. doi:10.2989/AJMS.2008.30.1.7.457.
785 Soetaert, K., Petzoldt, T., and Setzer, R.W. 2010. Solving Differential Equations in R: Package deSolve. J.
786 Stat. Softw. **33**(9): 1–25. doi:10.18637/jss.v033.i09.
787 Stock, B.C., and Miller, T.J. 2021. The Woods Hole Assessment Model (WHAM): A general state-space
788 assessment framework that incorporates time-and age-varying processes via random effects
789 and links to environmental covariates. Fish. Res. **240**: 105967.
790 Stock, B.C., Xu, H., Miller, T.J., Thorson, J.T., and Nye, J.A. 2021. Implementing two-dimensional
791 autocorrelation in either survival or natural mortality improves a state-space assessment model
792 for Southern New England-Mid Atlantic yellowtail flounder. Fish. Res. **237**: 105873.
793 doi:10.1016/j.fishres.2021.105873.
794 Thorson, J.T., Andrews III, A.G., Essington, T.E., and Large, S.I. 2024. Dynamic structural equation models
795 synthesize ecosystem dynamics constrained by ecological mechanisms. Methods Ecol. Evol.
796 **15**(4): 744–755. doi:10.1111/2041-210X.14289.
797 Thorson, J.T., Arimitsu, M.L., Barnett, L.A.K., Cheng, W., Eisner, L.B., Haynie, A.C., Hermann, A.J.,
798 Holsman, K., Kimmel, D.G., Lomas, M.W., Richar, J., and Siddon, E.C. 2021. Forecasting
799 community reassembly using climate-linked spatio-temporal ecosystem models. Ecography
800 **44**(4): 612–625. doi:https://doi.org/10.1111/ecog.05471.
801 Thorson, J.T., and Minto, C. 2015. Mixed effects: a unifying framework for statistical modelling in
802 fisheries biology. ICES J. Mar. Sci. J. Cons. **72**(5): 1245–1256. doi:10.1093/icesjms/fsu213.
803 de Valpine, P. 2002. Review of methods for fitting time-series models with process and observation
804 error and likelihood calculations for nonlinear, non-Gaussian state-space models. Bull. Mar. Sci.
805 **70**(2): 455–471.
806 Walters, C., Christensen, V., and Pauly, D. 1997. Structuring dynamic models of exploited ecosystems
807 from trophic mass-balance assessments. Rev. Fish Biol. Fish. **7**(2): 139–172.
808 doi:10.1023/A:1018479526149.
809 Walters, C., and Kitchell, J.F. 2001. Cultivation/depensation effects on juvenile survival and recruitment:
810 implications for the theory of fishing. Can. J. Fish. Aquat. Sci. **58**(1): 39–50.
811 Walters, C.J., Christensen, V., Martell, S.J., and Kitchell, J.F. 2005. Possible ecosystem impacts of applying
812 MSY policies from single-species assessment. ICES J. Mar. Sci. **62**(3): 558–568.
813 doi:10.1016/j.icesjms.2004.12.005.
814 Whitehouse, G.A., Aydin, K.Y., Hollowed, A.B., Holsman, K.K., Cheng, W., Faig, A., Haynie, A.C., Hermann,
815 A.J., Kearney, K.A., Punt, A.E., and Essington, T.E. 2021. Bottom–Up Impacts of Forecasted

816 Climate Change on the Eastern Bering Sea Food Web. Front. Mar. Sci. **8**. Frontiers.
817 doi:10.3389/fmars.2021.624301.
818 Winker, H., Carvalho, F., and Kapur, M. 2024. JABBA: Just Another Bayesian Biomass Assessment.
819 Available from https://github.com/jabbamodel/JABBA.
820 Winker, H., Carvalho, F., Thorson, J.T., Kell, L.T., Parker, D., Kapur, M., Sharma, R., Booth, A.J., and
821 Kerwath, S.E. 2020. JABBA-Select: Incorporating life history and fisheries' selectivity into surplus
822 production models. Fish. Res. **222**: 105355. doi:10.1016/j.fishres.2019.105355.
823 Xu, H., Thorson, J.T., and Methot, R.D. 2020. Comparing the performance of three data-weighting
824 methods when allowing for time-varying selectivity. Can. J. Fish. Aquat. Sci. **77**(2): 247–263.
825 doi:10.1139/cjfas-2019-0107.
826

827

828 Fig. 1: Estimated trophic level (y-axis) and pelagic proportions (x-axis) for the eastern Bering Sea
829 case study (top panel) or the simulation experiment (bottom panel). Taxa are labeled
830 alphabetically following their row-order in Table S2 and S3, respectively, with vertex circles
831 having size representing the log-mass of each variable, and the edges color-coded to represent the
832 log-consumption flowing from predator to prey. We compute "Pelagic proportion" by treating
833 "Pelagic prod." and "Producer" as the source of pelagic production in each model, respectively.

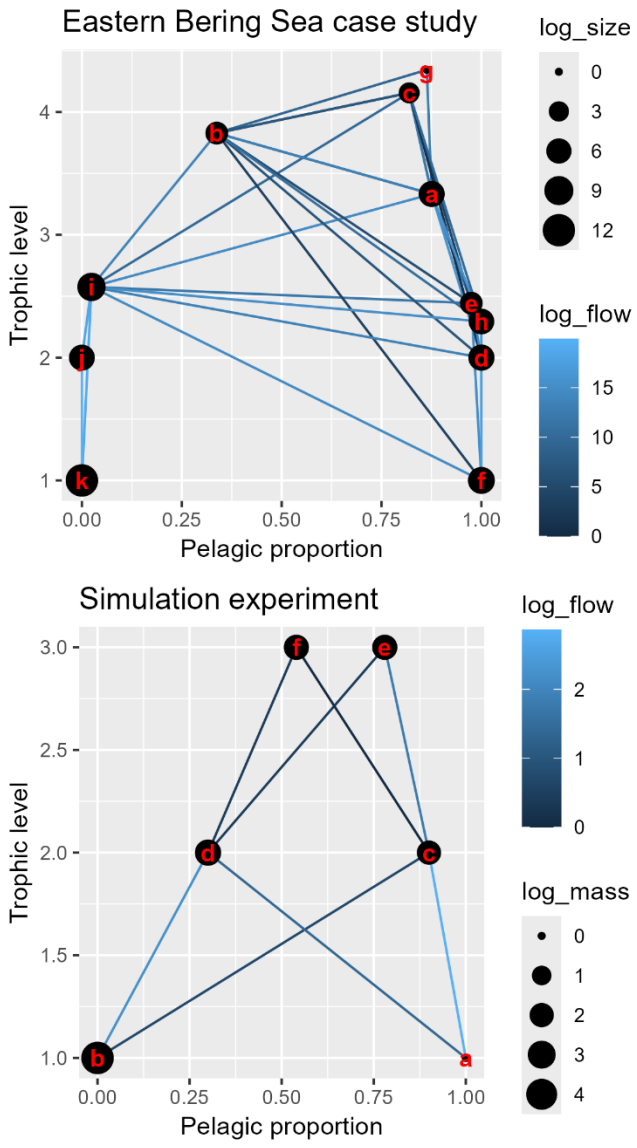

834

835

Fig. 2 – Estimated abundance (y-axis in teragrams a.k.a. million metric tons, black line) +/- one standard error (grey shaded ribbon) in each year (x-axis) for each modeled variable (panels), plotted against the indices of biomass (black dots) for cod, arrowtooth, northern fur seals, Pollock, Copepods, Other Zooplankton, Krill, and Primary producers. For pollock, we also show the raw index of biomass (x-symbols) and the index divided by the estimated catchability coefficient (black dots), to show the estimated biomass relative to the bottom-trawl survey scale. Note that Benthic invertebrates, Benthos, and Detritus have neither absolute nor relative abundance available.

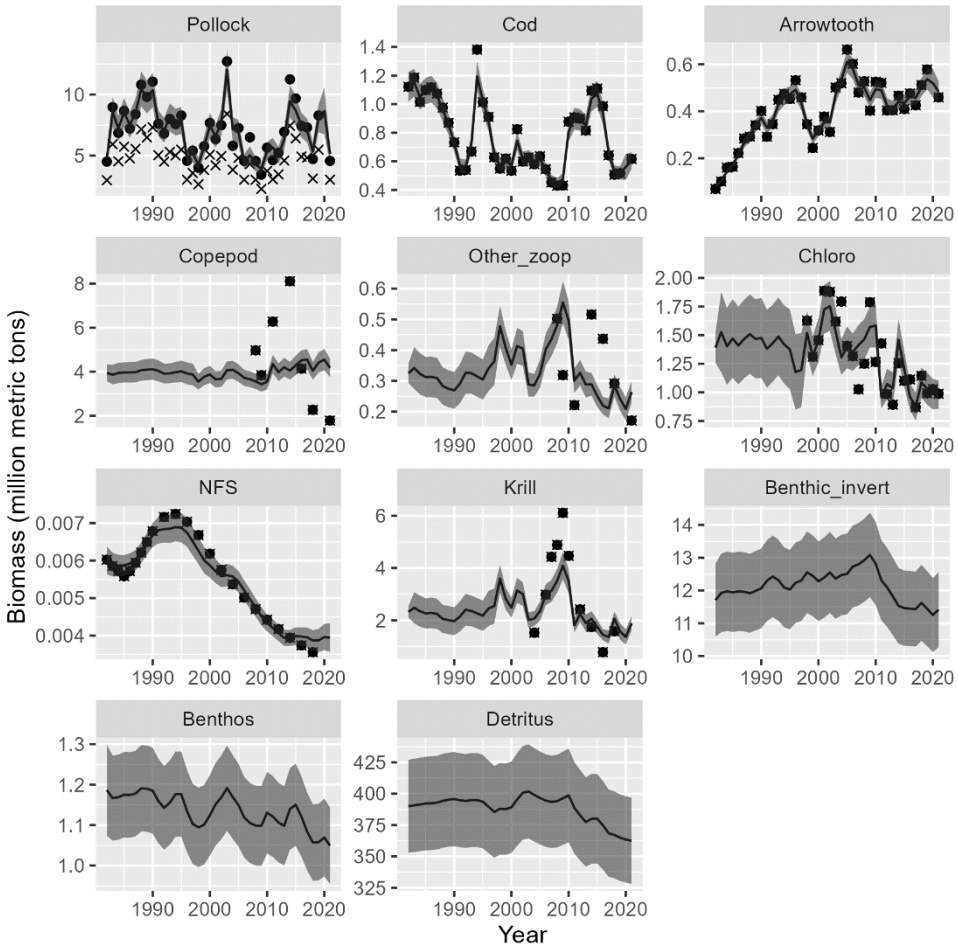

Fig. 3: Comparison of biomass estimates using the full model (black), a null model without process errors or catches (red), and a "measurement-error" model that includes catches but no process errors (blue), where each shows +/- one standard error as shading.

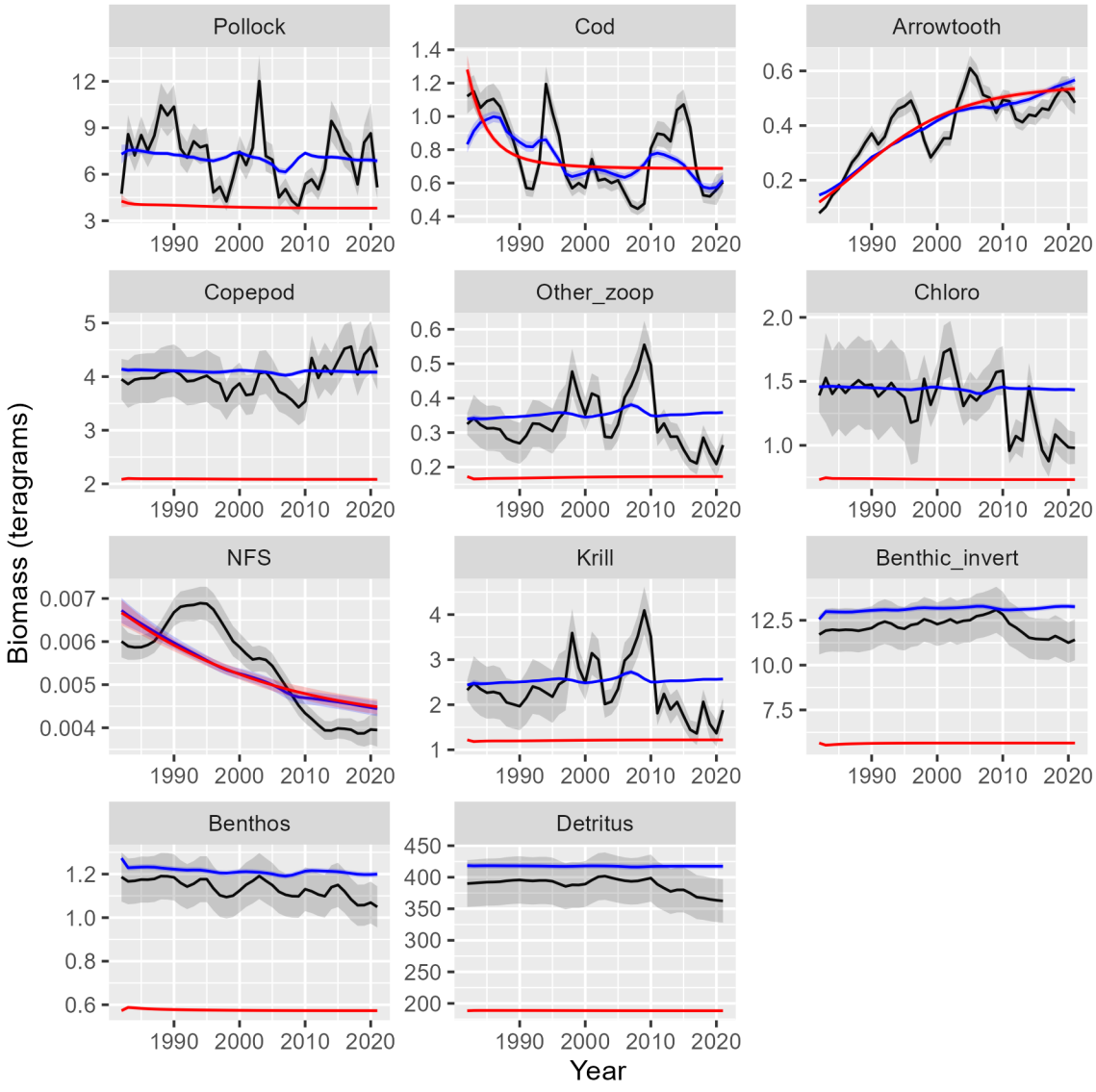

Fig. 4 – Estimated rates that affect productivity, i.e., $g(t)$ (production rate; green) and $m(t)$ (mortality rate including consumption; blue) for each modeled species in the eastern Bering Sea, as well as $f(t)$ (fishing mortality rate; red) for the three species with fishery catches, showing the predicted value (line) +/- 1 standard error (shaded area). Note that change in biomass $\frac{d}{dt}\beta(t) = \big(g(t) - f(t) - m(t) + \epsilon(t)\big) \times \beta(t)$ (where process error ϵ is plotted separately in Fig. S2) such that g has a positive effect while m and f have negative effects

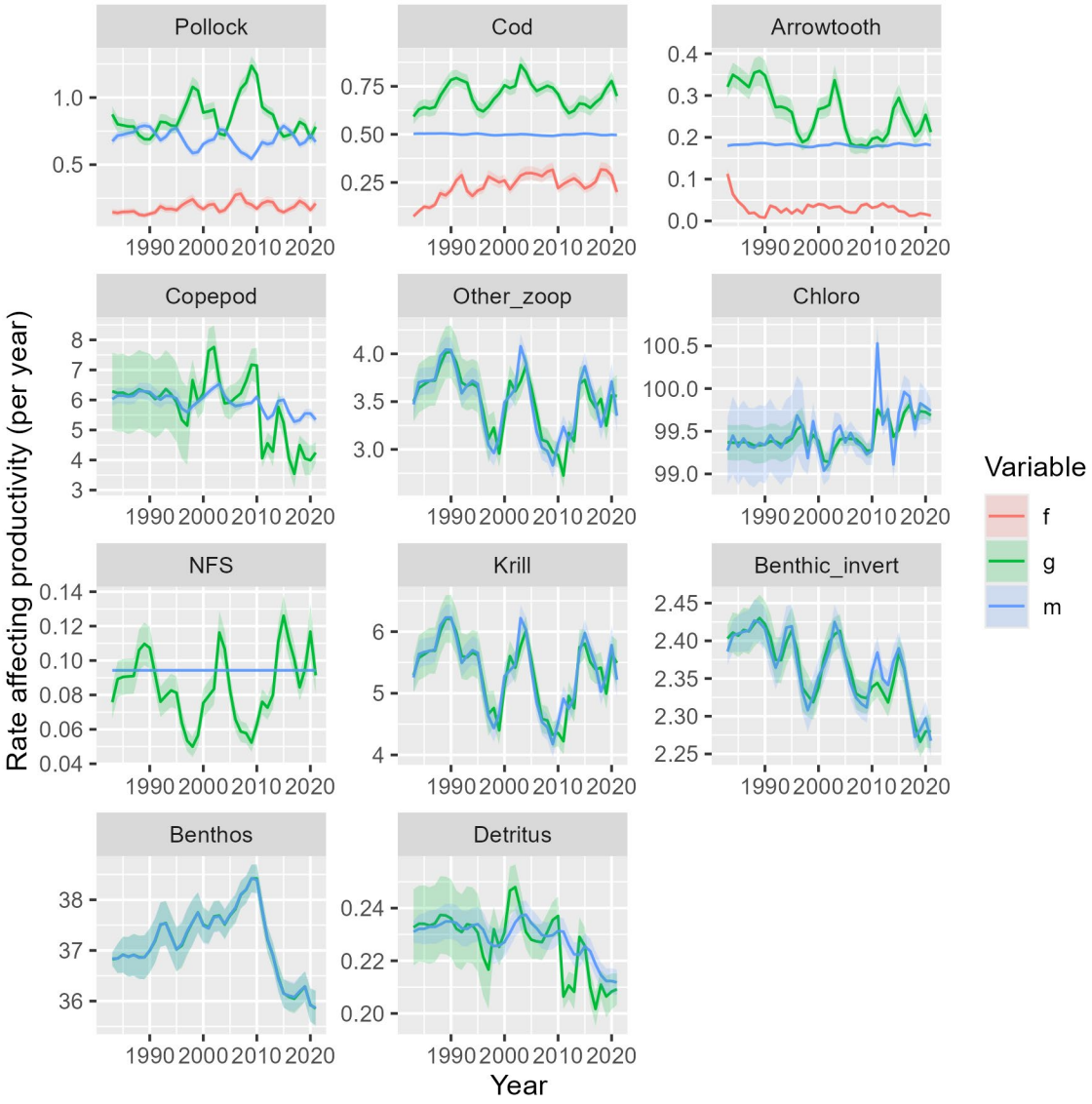

Fig. 5 – Stacked barplot showing growth rate $g(t)$ (left column) or natural mortality rate $m(t)$ (right column) for pollock (top row, i.e., matching green and blue lines in first panel of Fig. 3), cod (middle row, i.e., second panel of Fig. 3), and krill (bottom row, i.e., 8th panel of Fig. 3), while decomposing these demographic rates into the contribution for each prey species (i.e., each component of Eq. 5 for Growth) or for each predator species as well as a constant residual mortality rate (i.e., each component of Eq. 6 for Natural mortality), where $M0$ (pink) indicates residual natural mortality.

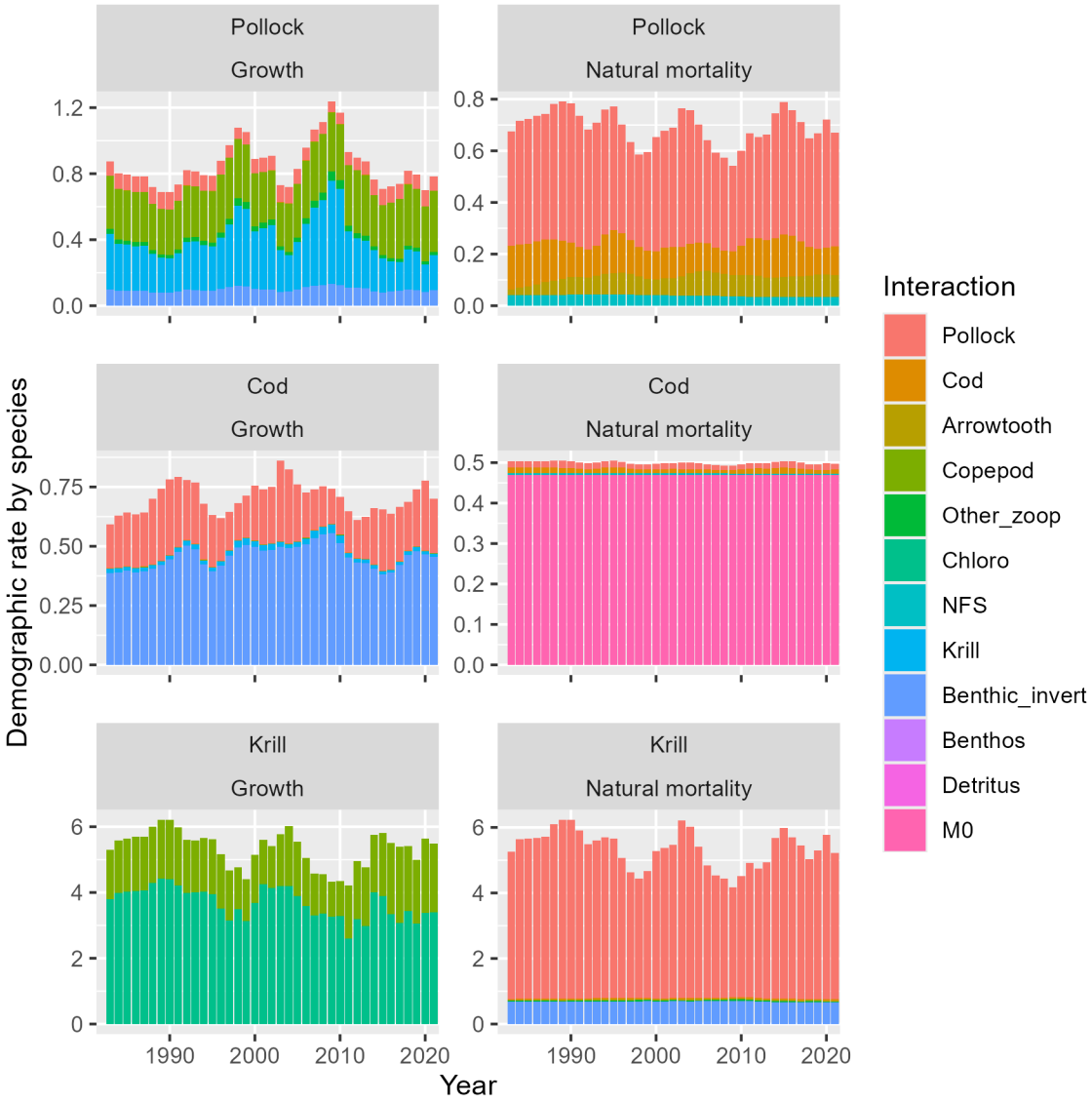

867 Fig. 6 – Range of errors that covers 10% and 90% of the 50 simulation replicates (y-axis) for
868 each year (x-axis) in annual estimates of growth from consumption (g), mortality due to
869 predation (m) (columns), or biomass (β) for each simulated species (rows) for either the state-
870 space model (red shading) or the same model but without estimating process errors in dynamics
871 (blue shading), and also showing the median error for both models (red and blue lines,
872 respectively). Note that the two predators (bottom two rows) experience no predation (see Table
873 S3) such that their mortality is specified without error and therefore not shown.

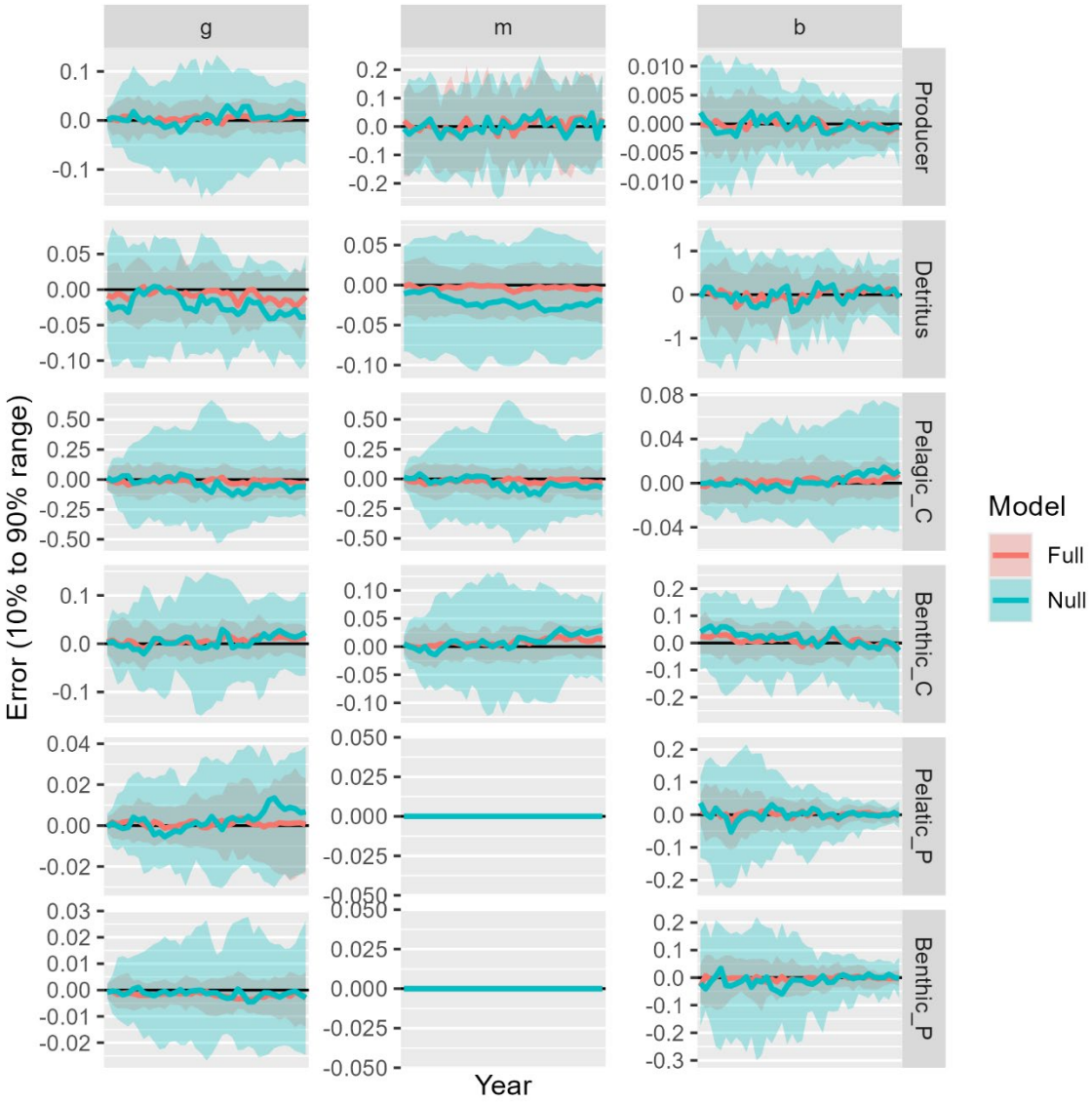

874

Supplementary Materials 1: Simplifying functional responses

In the main text, we present a formula for consumption (Eq. 4) that eliminates additional terms that can be used to represent ecological interactions among predators and prey. We follow default settings from Rpath (described in Lucey et al. (2020)), and only eliminate terms that are not used given those default values. Here, we summarize how Eq. 4 results from the default values used for these additional terms:

1. *Foraging time:* Ecosim can be configured to represent prey-specific foraging time. Lucey et al. (2020) defines prey-specific foraging time $Ftime_{i,m}$ (see Eq. 19-22 of that paper) and an adjustment rate $Fadj_i$. Their default is to start $Ftime_{i,m} = 1$ in the initial time, with adjustment rate $Fadj_i = 0$, such that $Ftime_{i,m} = 1$ for all subsequent times. As a result, prey-specific foraging time is constant, and this specification avoids integrating additional state variables. Lucey et al. (2020) states that the EwE software uses a default value of $Fadj_i = 0.5$, so EcoState does not correspond to the default values for the EwE software.
2. *Forcing functions*: Ecosim can be configured to include forcing functions, which represent unmodeled variation in consumption. We instead assume that these are captured in estimated process errors, and do not include the option in our definition of consumption.
3. *Prey functional response*: Ecosim can be configured to represent the prey functional response (third term of the right-hand-side of Eq. 4) using a parameter representing predator-specific handling time that controls the shape of the functional response. We again refer to notation from Lucey et al. (2020 Eq. 19-22), which defines predator-specific handling time parameter D_{ij} (which accounts for predator saturation as prey become abundant), and functional-response parameter θ ($\theta = 1$ results in a Holling's Type-2 and $\theta = 2$ results in a

Holling's Type-3 functional response). Their default is $D_{ij} = 1000$ and $\theta = 1$, and they note that "for practical use, values $D_{ij} > 1000$ are indistinguishable from infinity" for parameter D_{ij}. We therefore instead define $D_{ij} \to \infty$, where these values for D_{ij} and θ then simplify to the linear prey functional response that is included in the main text.

4. *Facilitation and multispecies functional response:* Ecosim includes parameters that control whether consumption for a given pair of predator and prey is affected the biomass of other predators or prey. This then represents e.g., facilitation or interference competition. Default values from Lucey et al. (2020) eliminate those responses, so we do not include them in Eq. 4 notation.

We recommend that future research explore the costs (e.g., computational time), benefits (e.g., ecological realism and stability), and trade-offs (e.g., statistical parsimony) that arise when adding these back in.

Works cited

Aydin, K., Gaichas, S., Ortiz, I., Kinzey, D., & Friday, N. (2007). *A comparison of the Bering Sea, Gulf of Alaska, and Aleutian Islands large marine ecosystems through food web modeling* (NOAA Tech. Memo. NMFS-AFSC-178; p. 298). U.S. Dep. Commer. https://repository.library.noaa.gov/view/noaa/22894/noaa_22894_DS1.pdf

Barbeaux, S. J., Barnett, L., Connor, J., Nielson, J., Shotwell, S. K., Siddon, E., Spies, I., Ressler, H. R., Rohan, S., & Sweeney, K. (2022). Assessment of the Pacific cod stock in the Eastern Bering Sea. *Stock Assessment and Fishery Evaluation Report for the Groundfish Resources of the Bering Sea and Aleutian Islands. North Pacific Fishery Management Council*, *1007*. https://apps-afsc.fisheries.noaa.gov/plan_team/2022/EBSpcod.pdf

Barlow, J., & Boveng, P. (1991). MODELING AGE-SPECIFIC MORTALITY FOR MARINE MAMMAL POPULATIONS. *Marine Mammal Science*, *7*(1), 50–65. https://doi.org/10.1111/j.1748-7692.1991.tb00550.x

Brown, Z. W., Dijken, G. L. van, & Arrigo, K. R. (2011). A reassessment of primary production and environmental change in the Bering Sea. *Journal of Geophysical Research: Oceans*, *116*(C8). https://doi.org/10.1029/2010JC006766

Choquet, M., Kosobokova, K., Kwaśniewski, S., Hatlebakk, M., Dhanasiri, A. K. S., Melle, W., Daase, M., Svensen, C., Søreide, J. E., & Hoarau, G. (2018). Can morphology reliably distinguish between the copepods Calanus finmarchicus and C. glacialis, or is DNA the only way? *Limnology and Oceanography: Methods*, *16*(4), 237–252. https://doi.org/10.1002/lom3.10240

Edwards, A. M., & Auger-Méthé, M. (2019). Some guidance on using mathematical notation in ecology. *Methods in Ecology and Evolution*, *10*(1), 92–99. https://doi.org/10.1111/2041-210X.13105

Frost, B. W. (1974). Calanus marshallae, a new species of calanoid copepod closely allied to the sibling species C. finmarchicus and C. glacialis. *Marine Biology*, *26*(1), 77–99. https://doi.org/10.1007/BF00389089

Ianelli, J. N., Stienessen, S., Honkalehto, T., Siddon, E., & Allen-Akselrud, C. (2022). *Assessment of the walleye pollock stock in the Eastern Bering Sea* [NPFMC Bering Sea and Aleutian Islands SAFE]. North Pacific Fishery Management Council.

Incze, L. S., Siefert, D. W., & Napp, J. M. (1997). Mesozooplankton of Shelikof Strait, Alaska: Abundance and community composition. *Continental Shelf Research*, *17*(3), 287–305. https://doi.org/10.1016/S0278-4343(96)00036-2

Kimmel, D. G., & Duffy-Anderson, J. T. (2020). Zooplankton abundance trends and patterns in Shelikof Strait, western Gulf of Alaska, USA, 1990–2017. *Journal of Plankton Research*, *42*(3), 334–354. https://doi.org/10.1093/plankt/fbaa019

Livingston, P. A., Aydin, K., Buckley, T. W., Lang, G. M., Yang, M.-S., & Miller, B. S. (2017). Quantifying food web interactions in the North Pacific – a data-based approach. *Environmental Biology of Fishes*, *100*(4), 443–470. https://doi.org/10.1007/s10641-017-0587-0

Lucey, S. M., Gaichas, S. K., & Aydin, K. Y. (2020). Conducting reproducible ecosystem modeling using the open source mass balance model Rpath. *Ecological Modelling*, *427*, 109057. https://doi.org/10.1016/j.ecolmodel.2020.109057

Maritorena, S., d'Andon, O. H. F., Mangin, A., & Siegel, D. A. (2010). Merged satellite ocean color data products using a bio-optical model: Characteristics, benefits and issues. *Remote Sensing of Environment*, *114*(8), 1791–1804.

Markowitz, E. H., Dawson, E. J., Charriere, N. E., Prohaska, B. K., Rohan, S. K., Stevenson, D. E., & Britt, L. L. (2022). *Results of the 2021 eastern and northern Bering Sea continental shelf bottom trawl survey of groundfish and invertebrate fauna*. https://repository.library.noaa.gov/view/noaa/47710

McHuron, E.A., Luxa, K., Pelland, N.A., Holsman, K., Ream, R.R., Zeppelin, T.K., & Sterling J.T. (2020). Practical Application of a Bioenergetic Model to Inform Management of a Declining Fur Seal Population and Their Commercially Important Prey. *Frontiers in Marine Science*. https://doi.org/10.3389/fmars.2020.597973

Miller, C. B. (1988). *Neocalanus flemingeri*, a new species of Calanidae (Copepoda: Calanoida) from the subarctic Pacific Ocean, with a comparative redescription of *Neocalanus plumchrus* (Marukawa) 1921. *Progress in Oceanography*, *20*(4), 223–273. https://doi.org/10.1016/0079-6611(88)90042-0

Napp, Jeffrey. M., Incze, L. S., Ortner, P. B., Siefert, D. L. W., & Britt, L. (1996). The plankton of Shelikof Strait, Alaska: Standing stock, production, mesoscale variability and their relevance to larval fish survival. *Fisheries Oceanography*, *5*(s1), 19–38. https://doi.org/10.1111/j.1365-2419.1996.tb00080.x

Polovina, J. J. (1984). Model of a coral reef ecosystem. *Coral Reefs*, *3*(1), 1–11. https://doi.org/10.1007/BF00306135

Ressler, P. H., De Robertis, A., Warren, J. D., Smith, J. N., & Kotwicki, S. (2012). Developing an acoustic survey of euphausiids to understand trophic interactions in the Bering Sea

ecosystem. *Deep Sea Research Part II: Topical Studies in Oceanography*, *65–70*, 184–195. https://doi.org/10.1016/j.dsr2.2012.02.015

Shotwell, S. K., Spies, I., Brit, L., Bryan, M., Hanselman, D. H., Nichol, D. G., Hoff, J., Palsson, W., Siwicke, K., & Wilderbuer, T. K. (2021). Assessment of the arrowtooth flounder stock in the Bering Sea and Aleutian Islands. *Stock Assessment and Fishery Evaluation Report for the Groundfish Resources of the Bering Sea and Aleutian Islands. North Pacific Fishery Mngt. Council, Anchorage, AK*, *99501*. https://apps-afsc.fisheries.noaa.gov/Plan_Team/2023/BSAIatf.pdf

Siler, W. (1979). A Competing-Risk Model for Animal Mortality. *Ecology*, *60*(4), 750–757. https://doi.org/10.2307/1936612

Sullaway, G. (In revisions). *Evaluating the Performance of a System Model in Predicting Zooplankton Dynamics: Insights from the Bering Sea Ecosystem*.

Tarrant, A. M., Eisner, L. B., & Kimmel, D. G. (2021). Lipid-related gene expression and sensitivity to starvation in Calanus glacialis in the eastern Bering Sea. *Marine Ecology Progress Series*, *674*, 73–88. https://doi.org/10.3354/meps13820

Trites, A. W., & Bigg, M. A. (1996). Physical growth of northern fur seals (Callorhinus ursinus): Seasonal fluctuations and migratory influences. *Journal of Zoology*, *238*(3), 459–482. https://doi.org/10.1111/j.1469-7998.1996.tb05406.x

Walters, C., Christensen, V., & Pauly, D. (1997). Structuring dynamic models of exploited ecosystems from trophic mass-balance assessments. *Reviews in Fish Biology and Fisheries*, *7*(2), 139–172. https://doi.org/10.1023/A:1018479526149

Whitehouse, G. A., Aydin, K. Y., Hollowed, A. B., Holsman, K. K., Cheng, W., Faig, A., Haynie, A. C., Hermann, A. J., Kearney, K. A., Punt, A. E., & Essington, T. E. (2021). Bottom–Up Impacts of Forecasted Climate Change on the Eastern Bering Sea Food Web. *Frontiers in Marine Science*, *8*. https://doi.org/10.3389/fmars.2021.624301

Wiebe, P. H. (1975). Relationships between zooplankton displacement volume, wet weight, dry weight and carbon. *Fish. Bull.*, *73*, 777–786.

Wiebe, P. H. (1988). Functional regression equations for zooplankton displacement volume, wet weight, dry weight, and carbon: A correction. *Fisheries Bulletin*, *86*, 833–835.

Supplementary Materials 2: Solving for scale for each taxon

For each taxon s, the user must choose whether to treat equilibrium biomass $\bar{\beta}_s$ or ecotrophic efficiency e_s as a parameter for that taxon. A different choice can be made for each taxon, and EcoState then solves for the unspecified value for each taxon (e.g., solves for e_s if $\bar{\beta}_s$ is specified for taxon s). The user can specify one (but not both) of $\bar{\beta}_s$ and e_s for any single taxon, and at least one taxon must have $\bar{\beta}_s$ to avoid a degenerate solution of $\overline{\boldsymbol{\beta}} = \mathbf{0}$ (Polovina, 1984). This algorithm is included in Rpath (Lucey et al., 2020), but we repeat it here using notation from EcoState for readers who are not familiar with the algorithm.

Specifically, we define indicator a_s as:

$$a_s = \begin{cases} 0 & \text{if } \beta_s \text{ is specified} \\ 1 & \text{if } e_s \text{ is specified} \end{cases}$$

such that EcoState will treat $\overline{\boldsymbol{\beta}}_{\{\mathbf{a}=0\}}$ and $\mathbf{e}_{\{\mathbf{a}=1\}}$ as specified values and will solve for the value of $\overline{\boldsymbol{\beta}}_{\{\mathbf{a}=1\}}$ and $\mathbf{e}_{\{\mathbf{a}=0\}}$. We first calculate consumption $\tilde{c}_i$ for each prey i given any specified values of $\bar{\beta}_j$ for predators j:

$$\tilde{c}_i = \sum_{j \in \{\mathbf{a}=1\}} \beta_j d_{i,j}$$

We next define a vector that includes all specified values multiplied by production per biomass, $\mathbf{x} = \mathbf{p} \odot \left((\mathbf{1} - \mathbf{a}) \odot \overline{\boldsymbol{\beta}} + \mathbf{a} \odot \mathbf{e}\right)$, and define the matrix of prey-consumption-per-predator biomass for those species where ecotrophic efficiency is specified, $\mathbf{Z} = \mathbf{D} \odot (\mathbf{1}\mathbf{w}^T) \odot (\mathbf{1}\mathbf{a}^T)$. We seek to solve for the unspecified values $\mathbf{y} = \mathbf{a} \odot \overline{\boldsymbol{\beta}} + (\mathbf{1} - \mathbf{a}) \odot \mathbf{e}$. To do so, we calculate:

$$\mathbf{y} = (\text{diag}(\mathbf{x}) - \mathbf{Z})^{-1}\tilde{\mathbf{c}}$$

where $\mathrm{diag}(\mathbf{x})$ is a diagonal matrix with diagonal elements of $\mathbf{x}$. We then plug $\mathbf{y}$ into the unknown values, $\overline{\boldsymbol{\beta}}_{\{\mathbf{a}=1\}} = \mathbf{y}_{\{\mathbf{a}=1\}}$ and $\mathbf{e}_{\{\mathbf{a}=0\}} = \mathbf{y}_{\{\mathbf{a}=0\}}$.

Supplementary Materials 3: Data standardization

Zooplankton Sampling and Data Processing

Zooplankton was collected using oblique tows of paired bongo nets (20 cm frame, 153 μm mesh and 60 cm frame, 333 or 505 μm mesh) (Incze et al., 1997; Napp et al., 1996). The tows were within 5-10 m of the bottom depending on sea state and depth was monitored continuously using a SeaBird FastCAT CTD. Volume filtered was estimated using a General Oceanics flowmeter mounted inside the mouth of each net. Samples were preserved in 5% buffered formalin/seawater. Whole sample displacement volumes were estimated by first concentrating all animals onto a sieve using a small mesh size (53 μm) and all water was allowed to drain from the sieve. The animals are then added to a graduated cylinder of known volume and the difference in volume was recorded in mL. Zooplankton were identified to the lowest taxonomic level and stage possible at the Plankton Sorting and Identification Center in Szczecin, Poland, and verified at the Alaska Fisheries Science Center, Seattle, Washington, USA. A methodological change in zooplankton collection occurred in 2012, when the 60 cm frame net had its mesh changed to 505 μm. The majority of taxa were not affected by this change; however, the potential for some differences to arise were noted, see Kimmel and Duffy-Anderson (2020) for details.

Biomass was estimated for whole samples by converting the displacement volume (mL) to biomass using literature equations (Wiebe et al. 1975, Wiebe 1988). Biomass estimates for individual species were calculated from abundance (ind m^{-3}) estimates. Individual stage weight (wet mass) was estimated from laboratory measurements for *Calanus marshallae/glacialis*, *Neocalanus* spp. (*N. plumchrus* and *N. flemingeri* combined), and *N. cristatus* (Hopcroft unpub.) (Sullaway, In revisions). Note that the ability to distinguish between these *Calanus* species

morphologically is based on taxonomic characters that require significant processing time (Frost, 1974). This appears to be a problem across the genus as it has been suggested that the ability to distinguish between *C. glacialis* and *C. finmarchicus* in Atlantic waters can only be accomplished with DNA methods (Choquet et al., 2018). Recent results suggest that most *Calanus* spp. in the Bering Sea may in fact be *C. glacialis* (Tarrant et al., 2021). Similarly, *N. flemingeri* and *N. plumchrus* are closely related species in both size and mass (Miller, 1988); therefore, these two species were not distinguished in this analysis. Individual masses for the following stages were then summed for each sampling event to produce a single biomass estimate for copepodite stages C1-C6, with C6 being the adult stage. Wet mass was converted to dry mass or carbon using literature equations (Wiebe, 1975, 1988). Total large copepod biomass was then substracted from the whole sample biomasses to remove that contributing fraction to produce the large copepod and the other zooplankton biomass time-series.

Northern Fur Seals

Northern fur seal pups have been routinely counted on the Pribilof Islands (St. Paul Island, St. George Island) since the 1950s. From 1982 to 1992, pup counts were largely conducted annually on St. Paul Island and biennially on St. George Island, whereas from 1992 onwards they were largely biennial on both islands. Counts of the entire population are not possible because at any given time a certain proportion of the population is at sea. The Pribilof Island population has been in decline since the mid-to-late 1990s, primarily driven by declines on St. Paul Island, although it is unknown which component of the population is driving the decline. To estimate population size, we used the modeling approach described in McHuron et al. (2020), which resulted in a total of 11 different estimates of numbers at age for male and female fur seals. Animals <2 years of age were not included in population estimates since pups predominately rely

on milk from their mother while in the eastern Bering Sea, and once they depart on their post-weaning migration, most pups do not return until two years of age. See Supplementary Text in McHuron et al. (2020) for a more complete description. Population biomass in each year was estimated by multiplying the numbers at age for each sex (averaged across all 11 models) with age-sex specific mass estimates (Trites & Bigg, 1996) and then summing across all age and sex classes. The resulting population estimate was multiplied by ca. 30% to account for the fact that fur seals are seasonal residents of the eastern Bering Sea, spending on average of 105 - 109 days foraging in the model area. We only used biomass estimates from years where empirical estimates of pup production were available.

Ecopath parameters

Estimates of production per biomass (p_s and called P/B elsewhere), consumption per biomass (w_s and called Q/B elsewhere), and diet composition were derived from previous Ecopath with Ecosim models for the eastern Bering Sea. Detailed parameter estimation methods for all EBS EwE functional groups can be found in Aydin et al. (2007). Specifically:

- *Groundfish groups* combined mortality estimates from the literature and stock assessments with growth information available from field studies or the literature. Groundfish diet compositions were obtained from the NOAA/AFSC groundfish food habits monitoring program (Livingston et al., 2017). The groundfish diet compositions were combined across predator size classes by taking the weighted average of age-specific consumption, weighted by the product of abundance-at-age from stock assessments, size-at-age from assumed growth functions, and ration-at-size from bioenergetic models.
- *Northern fur seal* production was estimated with Siler's (1979) competing risk model as modified by Barlow and Boveng (1991) to construct a general model of survivorship. The

northern fur seal diet composition was compiled from the literature. However, we substitute a bioenergetic calculation for consumption per biomass based on a recently published bioenergetic model (McHuron unpublished work), which corrected for seasonal residency in the modeled area;

- *Zooplankton* production rates and diet compositions were estimated from values reported in the literature. The copepod consumption rate was retrieved from the literature, while the consumption of euphausiids and other zooplankton was estimated with an assumed growth efficiency.
- *Benthic invertebrate* production rates were from the literature and consumption was estimated with an assumed growth efficiency. Estimates of P/B and Q/B for commercial crabs were derived from stock assessment information. Benthic invertebrate diet compositions were derived from literature sources. The production of benthic microbes were derived from literature values for pelagic microbes. The Q/B of benthic microbes was estimated assuming a growth efficiency of 0.35, and the diet composition was assumed to consist entirely of detritus.

We then aggregated multiple groups to create the variables used here. This aggregation is done by taking the biomass-weighted average of production per biomass p_s, consumption per biomass w_s, and diet proportions $d_{i,j}$ across multiple taxa from Whitehouse et al. (2021). Pollock, cod, arrowtooth, and northern fur seal all aggregated juvenile and adult stages from Whitehouse et al. (2021). Similarly, Chloro included large and small phytoplankton, and Benthic_invert included tanner, snow, and king crabs, pandalid shrimps, benthic zooplankton, motile epifauna, structural epifauna, and infauna. The biomass variables from Whitehouse et al. (2021) that are aggregated into our 10 biomass variables (i.e., excluding detritus) represents 79% of the total biomass from

Whitehouse et al. (2021). The diet-composition matrix was then rescaled to ensure that each predator had proportions that summed to one.

Primary producers

Satellite chlorophyll-*a* concentration data from 1998 to 2023 for the southern (<60 N) Bering Sea middle and outer shelf (50-180 m bottom depth) were used to calculate annual time series trends. We compiled 8-day satellite chlorophyll-*a* concentration (ug l^{-1}) at a 4 km-resolution from The Hermes GlobColour website: http://hermes.acri.fr/ (Maritorena et al., 2010). This product is a standardized merged chlorophyll-*a* product, combining remote sensing data from SeaWiFS, MERIS, MODIS, VIIRS and OLCI. chlorophyll-*a* concentration data. Data were averaged for the months May to October for the middle and outer southern Bering Sea shelf region. Chlorophyll-*a* concentration data from locations near river plumes from the Yukon and Kuskowim rivers can be highly uncertain and were excluded, following recommendations in Brown et al. (2011).

Supplementary Materials 4: Additional tables and figures

Table S1: Notation used in the model presentation and results, including the symbol, units, a brief description, and the type. Note that notation differs from past Ecopath-with-Ecosim standards, to avoid using multiple symbols to indicate a single variable (Edwards & Auger-Méthé, 2019).

Symbol	Units	Description	Type
s	-	Species	Index
i	-	Prey	Index
j	-	Predator	Index
t	-	Time index	Index
k	-	Fishery	Index
$h_s(t)$	$Mass$	Catch for each species s and time t	Data
$b_s(t)$	$Mass$	Biomass index	Data
p_s	$Time^{-1}$	Production rate per biomass (elsewhere called PB)	Specified
w_s	$Time^{-1}$	Consumption rate per biomass (elsewhere called QB)	Specified
$x_{i,j}$	$Unitless$	Vulnerability for prey s_2 to predator s_1 (called X_{ij} in Walters et al. (1997))	Specified
$d_{i,j}$	$Unitless$	Diet fraction for prey s_2 and predator s_1	Specified
$r_{s,f}$	$Unitless$	Selectivity ratio for each species s in a given fishery f	Specified
σ_s^2	$Unitless$	Measurement error variance for biomass indices	Specified
v_s^2	$Unitless$	Measurement error variance for catch data	Specified
$y_s(t)$	$Time^{-1}$	Tracer release for taxa s	Specified
$\bar{\beta}_s$	$Mass$	Equilibrium biomass	Estimated
$\phi_k(t)$	$Time^{-1}$	Annual fishing mortality rate	Estimated
q_s	$Unitless$	Catchability coefficient for species s	Estimated
δ_s	$Unitless$	Difference between biomass and equilibrium biomass in the initial time	Estimated
τ_s^2	$Unitless$	Process error variance for biomass dynamics	Estimated
$\epsilon_s(t)$	$Time^{-1}$	Process error variation	Estimated
$\beta_s(t)$	$Mass$	Modeled biomass	Derived
$\eta_s(t)$	$Mass$	Modeled catch	Derived
$g_s(t)$	$Time^{-1}$	Growth rate	Derived
e_s	$Time^{-1}$	Ecotrophic efficiency	Derived
v_s	$Time^{-1}$	Detritus export (a.k.a. turnover) rate	Derived
u_s	$Time^{-1}$	Unmodeled mortality rate (elsewhere called $M0$)	Derived
$c_{i,j}(t)$	$Time^{-1}$	Consumption for each prey s_2 and predator s_1	Derived
$\bar{c}_{i,j}$	$Time^{-1}$	Equilibrium consumption	Derived
$g_s(t)$	$Time^{-1}$	Growth rate per biomass	Derived
$m_s(t)$	$Time^{-1}$	Natural mortality rate per biomass	Derived
$f_s(t)$	$Time^{-1}$	Fishing mortality rate per biomass	Derived
$z_s(t)$	$Unitless$	Tracer concentration for predator s	Derived

1144 Table S2: Data sets used for fitting the eastern Bering Sea case study

Data set	Years covered	Details	Reference
Cod, pollock, and arrowtooth biomass	1982-2023 (annual)	Using the design-based biomass index from a summer bottom trawl survey	(Markowitz et al., 2022)
Copepod and Other pelagic zooplankton biomass index	2008, 2009, 2011, 2014, 2016, 2018, 2021, 2022	From an oblique-tow small-mesh pelagic trawl, averaging Spring (May) and Fall (September) densities	(Incze et al., 1997; Kimmel & Duffy-Anderson, 2020)
Primary production biomass index	1998-2023 (annual)	From satellite chlorophyll-*a* concentration measurements, averaged from May through October of each year	
Krill biomass	2004, 2006-2010, 2012, 2014, 2016, 2018, 2022	From summer acoustic-midwater trawl survey	(Ressler et al., 2012)
Northern fur seal biomass	1982-2018 (biennial after 1990)		(McHuron et al., 2020)
Total catch biomass for cod, pollock, and arrowtooth	1982-2023 (annual)	From stock assessments	(Barbeaux et al., 2022; Ianelli et al., 2022; Shotwell et al., 2021)
Ecopath parameters and diet matrix	NA	From previous Rpath model	(Aydin et al., 2007; Whitehouse et al., 2021)

1145

Table S3: Ecopath parameters (rows) specified or calculated for each taxa (column) in the eastern Bering Sea case study (see Table S1 for units, where $Mass$ is using million metric tons and $Time$ is using years), and also showing diet proportions for prey (rows) given each taxa as predator (columns). Note that cod, arrowtooth, and northern fur seal (NFS) estimate equilibrium biomass $\bar{\beta}_s$ given the assumption that their catchability coefficient $q_s = 1$, and ecotrophic efficiency e_s is calculated to match that value. For other species, we specify ecotrophic efficiency $e_s = 1$ and equilibrium biomass $\bar{\beta}_s$ is calculated to match that value.

		Pollock	Cod	Arrow.	Copepod	Other zoop.	Pelagic prod.	NFS	Krill	Benthic invert	Benthic microbes	Detritus
Parameter or derived quantity	type	hetero	hetero	hetero	hetero	hetero	auto	hetero	hetero	hetero	hetero	detritus
	w_s	4.226	2.745	1.201	27.74	10.19	NA	57.764	15.64	11.912	104.29	NA
	p_s	0.825	0.507	0.186	6	3.57	99.407	0.094	5.48	2.43	36.5	0.5
	$\bar{\beta}_s$	7.186	1.639	0.896	3.95	0.325	1.39	0.005	2.324	11.706	1.186	390.038
	e_s	1	0.073	0.176	1	1	1	0	1	1	1	1
	u_s	0.2	0.2	0.2	0.2	0.2	0.2	0.2	0.2	0.2	0.2	0.2
	Trophic level	3.332	3.828	4.156	2	2.443	1	4.344	2.294	2.576	2	1
	Pelagic prop.	0.876	0.338	0.819	1	0.975	1	0.863	1	0.024	0	0
Prey proportions (d_{s_2,s_1})	Pollock	0.109	0.332	0.8	0	0	0	0.977	0	0	0	0
	Cod	0.001	0.007	0	0	0	0	0.023	0	0	0	0
	Arrowtooth	0.001	0.001	0.004	0	0	0	0	0	0	0	0
	Copepod	0.388	0.001	0	0	0.301	0	0	0.294	0.002	0	0
	Other zoop.	0.033	0	0	0	0.049	0	0	0	0	0	0
	Pelagic prod.	0	0	0	1	0.6	0	0	0.706	0.007	0	0
	NFS	0	0	0	0	0	0	0	0	0	0	0
	Krill	0.357	0.028	0.113	0	0.025	0	0	0	0.011	0	0
	Ben. Invert	0.112	0.632	0.082	0	0.025	0	0	0	0.158	0	0
	Ben. microbe	0	0	0	0	0	0	0	0	0.311	0	0
	Detritus	0	0	0	0	0	0	0	0	0.511	1	0

Table S4: Ecopath parameters in the simulation experiment (see Table S2 caption for details)

		Producer	Detritus	Pelagic consumer	Benthic consumer	Pelagic predator	Benthic predator
Param	Type	auto	detritus	hetero	hetero	hetero	hetero
	w_s	NA	NA	10	4	3	1
	p_s	90	0.5	4	1	0.2	0.1
	$\bar{\beta}_s$	0.11	10.02	0.78	1.33	1	1
	e_s	0.9	0.9	0.9	0.9	0	0
	u_s	0.2	0.2	0.2	0.2	0.2	0.2
	Trophic level	1	1	2	2	3	3
	u_s	9	0.05	0.4	0.1	0.2	0.1
Prey proportions (d_{s_2,s_1})	Producer_1	0	0	0.9	0.3	0	0
	Producer_2	0	0	0.1	0.7	0	0
	Consumer_1	0	0	0	0	0.8	0.4
	Consumer_2	0	0	0	0	0.2	0.6
	Predator_1	0	0	0	0	0	0
	Predator_2	0	0	0	0	0	0

Table S5: List of estimated parameters and standard errors in the eastern Bering Sea case study, listing the parameter name (see definitions in Table S1), the Taxon s, the maximum likelihood estimator, and the standard error

Parameter	Taxon	Estimate	SE
$\log(\delta_s)$	Pollock	-0.416	0.124
	Cod	-0.38	0.159
	Arrowtooth	-2.424	0.267
	NFS	0.27	0.221
$\log(\bar{\beta}_s)$	Cod	0.494	0.123
	Arrowtooth	-0.11	0.247
	NFS	-5.385	0.2
$\log(\tau_s)$	Pollock	-1.128	0.141
	Cod	-1.591	0.148
	Arrowtooth	-1.997	0.192
	Copepod	0.128	0.169
	NFS	-3.259	0.35
$\log(q_s)$	Pollock	-0.412	0.109
	Copepod	0.102	0.104
	Chloro	4.836	0.124
	Other_zoop	1.848	0.098
	Krill	2.098	0.121

Fig. S1 – Simulated time-series (y-axis) for each year (x-axis) of growth $g(t)$ (left column), natural mortality $m(t)$ (middle column), or biomass $\beta(t)$ (right column) for each simulated taxa (rows).

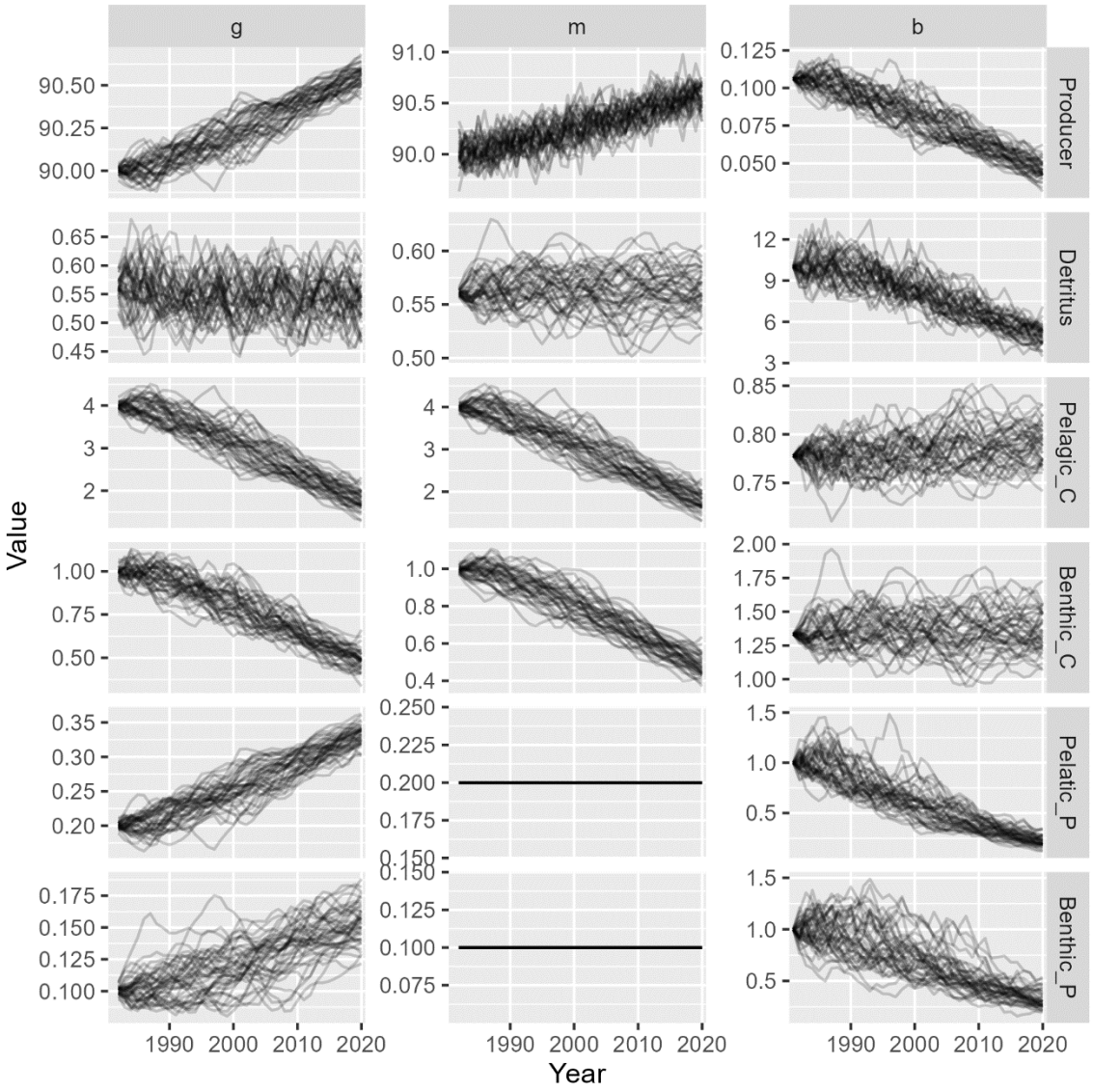

Fig. S2 – Fits to catch data for the three species with a directed fishery, showing predicted $\eta_s(t)$ (black line) +/- 1 standard error (grey shaded area) and observed catch $h_s(t)$ (black bullets).

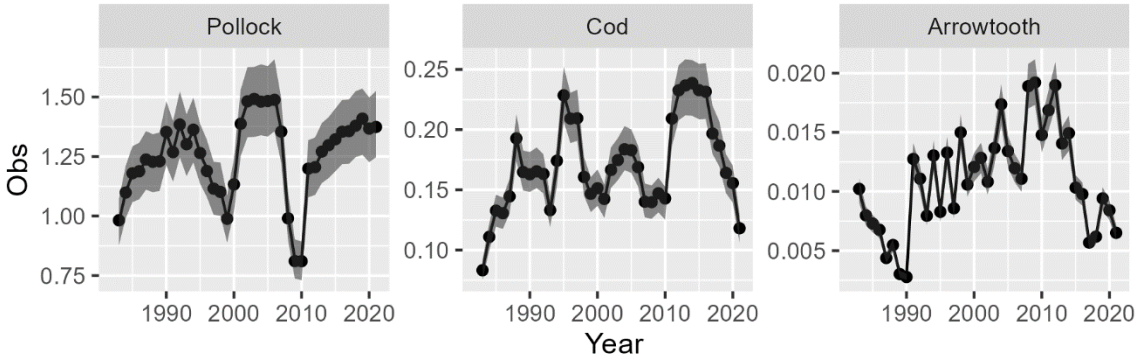

Fig. S3 – Annual estimates of process-error $\epsilon_s(t)$ (black lines) +/- 1 standard error (grey shaded area) for those species for which it is estimated.

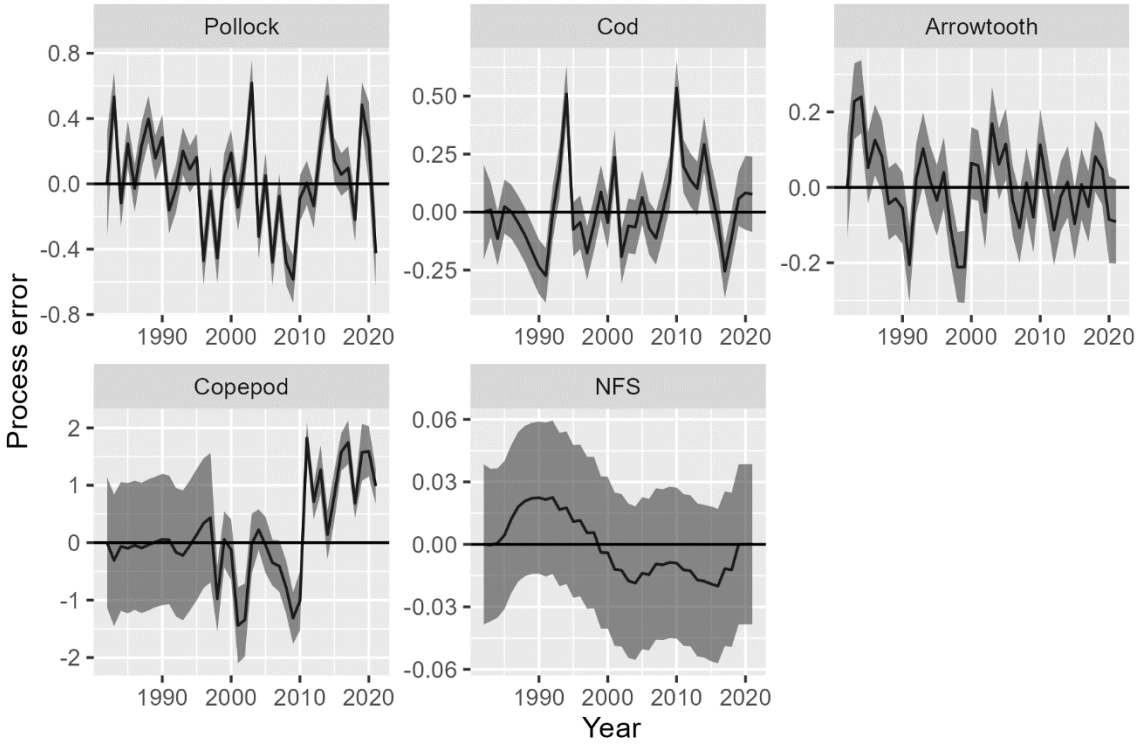

1173 Fig. S4: Equilibrium trophic level resulting from consumption rates in a given year for each
1174 modeled species (shaded area: +/- 1 standard error)

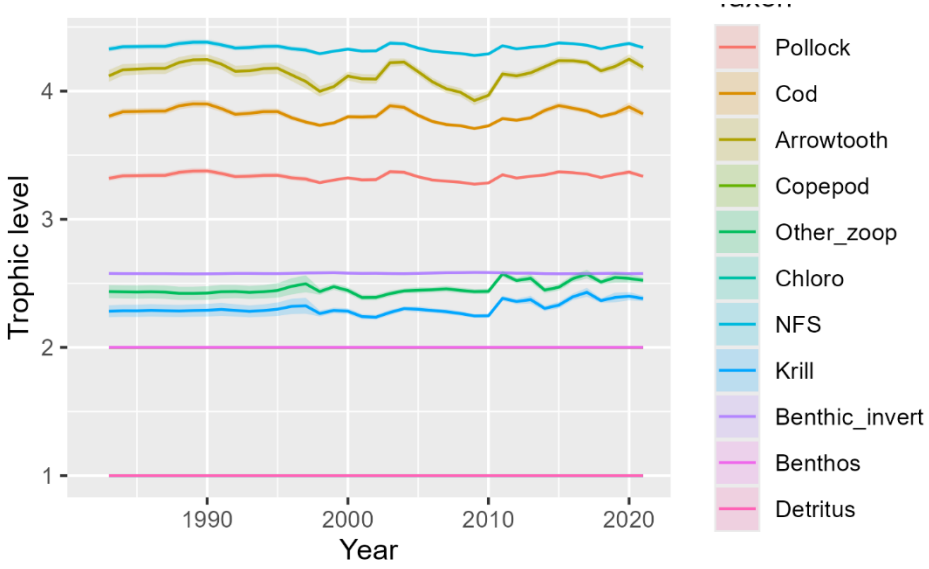

1175

1176

Fig. S5 – Performance (Box: 10% to 90% range; Line: mean) for estimated parameters in the simulation experiment, showing the true value (red), and estimates from the full (green) or null model (blue) for each of 13 parameters, where the single vulnerability parameter x_{shared} represents the predator-prey functional response for all predators and prey, $x_{shared} = 1 + \exp(Xprime\_ij)$ where $Xprime\_ij$ is the estimated parameter with unbounded support, and $Xprime\_ij$ is shown here. Note that the null model does not estimate process errors, and, therefore, has no value listed for the standard deviation of process errors (τ_s).

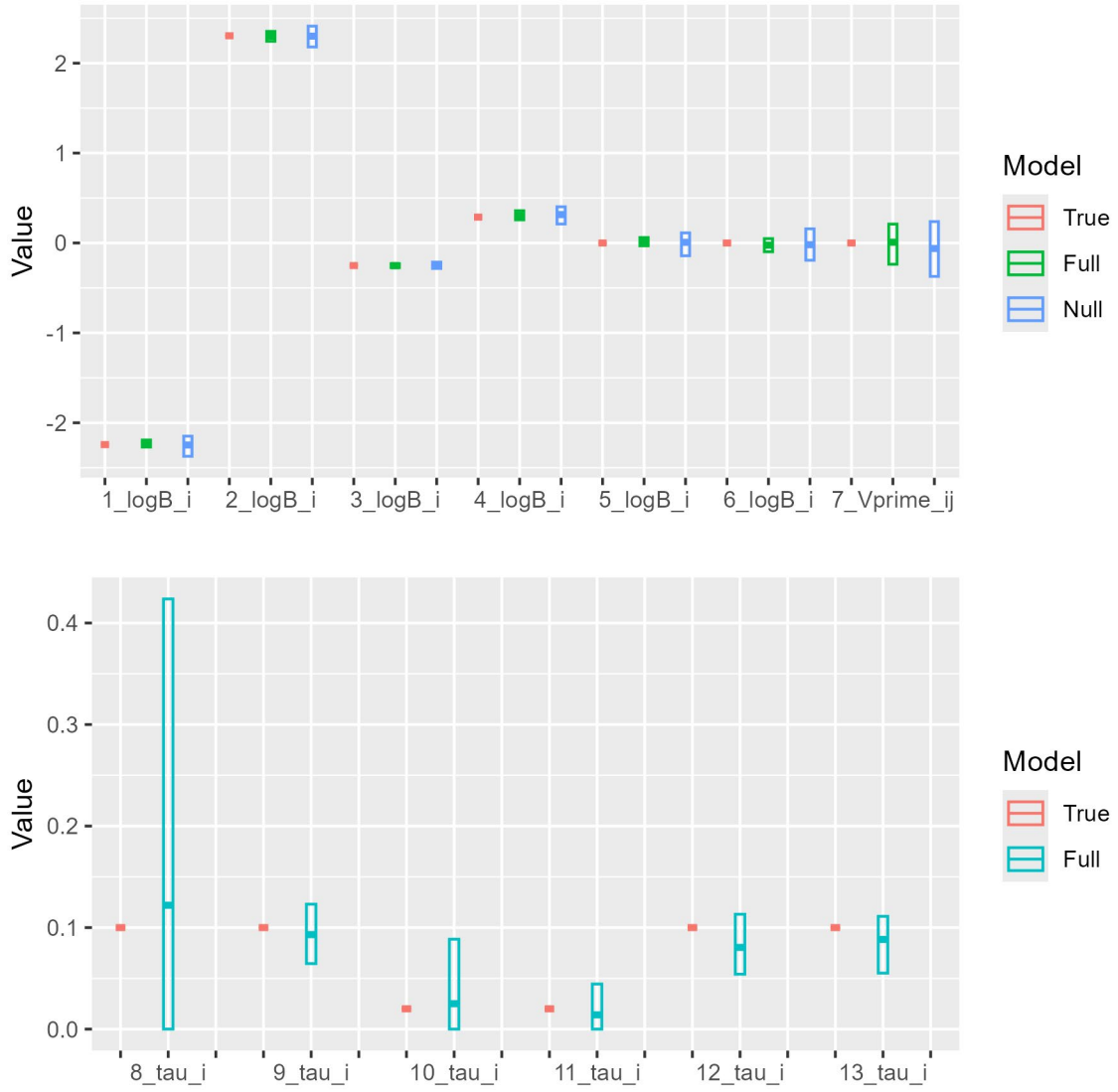

1187